An Approach to the Sediment Transport Problem From General Physics

GEOLOGICAL SURVEY PROFESSIONAL PAPER 422-I

An Approach to the Sediment Transport Problem From General Physics

By R. A. BAGNOLD

PHYSIOGRAPHIC AND HYDRAULIC STUDIES OF RIVERS

GEOLOGICAL SURVEY PROFESSIONAL PAPER 422-I

From considerations of energy balance and of mechanical equilibrium, a mathematical expression is derived relating the rates of sediment transport as bedload and as suspended load to the expenditure of power by a statistically steady flow of water

UNITED STATES GOVERNMENT PRINTING OFFICE, WASHINGTON : 1966

UNITED STATES DEPARTMENT OF THE INTERIOR

STEWART L. UDALL, *Secretary*

GEOLOGICAL SURVEY

William T. Pecora, *Director*

For sale by the Superintendent of Documents, U.S. Government Printing Office
Washington, D.C. 20402 - Price 35 cents (paper cover)

CONTENTS

ILLUSTRATIONS

TABLE

SYMBOLS

Symbol meanings preceded by † refer to quantities involving the gravity acceleration g. These quantities have ambiguous dimensions and values depending on the ambiguous definition of weight. In relations between such quantities, g cancels out and therefore has been omitted, leaving the quantities expressed in practical units. However, g is necessarily retained in relations between such quantities and, for example, velocities. The shear stress τ, for instance, is sometimes expressed as $\rho\, gdS$ and sometimes as $\rho\, dS$, according to the context. There is no real ambiguity, because all relations are dimensionally correct.

Meanings of dimensionless symbols are preceded by ‡.

Symbol	Where introduced	Meaning
b	I 14	‡Ratio $\bar{v}'/u_*$.
C'	19	‡Transport concentration by immersed weight.
C_0	9	‡Static bed concentration by volume $=(1-\text{porosity})$.
c	14	‡Flow coefficient $\bar{u}/u_*$.
D	7	Grain size.
d	5	Flow depth.
e_b	6	‡Bedload transport efficiency $=\frac{\text{bedload work rate}}{\text{stream power}}$.
e_c, e_s	7	‡Factors of e_b.
e_s	6	‡Suspension efficiency $=\frac{\text{suspension work rate}}{\text{steam power}}$.
f	14	‡Residual upward momentum flux, an internal fluid stress.
g	IV	Gravity acceleration.
G	10	‡Special Reynolds number for solids sheared in fluid $=\frac{D}{\eta}\sqrt{\frac{\sigma T}{\lambda}}$.
i	4	†Transport rate of solids by immersed weight per unit width $=\frac{\sigma-\rho}{\sigma} gj$.
I	I 4	†Transport rate of solids by immersed weight per whole width of flow $=\frac{\sigma-\rho}{\sigma} gJ$.
j	4	Transport rate of solids by dry mass per unit width.
J	4	†Transport rate of solids by dry mass per whole width of flow.
m	4	†Mass of transported solids over unit bed area.
m'	4	†Immersed weight is $m'g=\frac{\sigma-\rho}{\sigma} mg$.
P	4	Stress transmitted from solid to solid normal to the plane of shear.
p	17	‡Proportion of unity, by weight, of a given size grade in a sample of heterogeneous granular material.
Q	5	Discharge.
$\mathbf{R}$	7	‡Conventional Reynolds number for fluid flow.
S	5	‡Energy slope.
T	4	†Stress transmitted from solid to solid tangential to the plane of shear.
$\overline{U}$	4	Mean transport velocity of solids.
U'_c	7	Transport velocity, relative to ground, of a notional nongranular moving flow boundary.
$\bar{u}$	6	Mean flow velocity $=\frac{Q}{\text{cross-sectional area}}$.
$\bar{u}'$, $\bar{v}'$, $\bar{w}'$	13	Root-mean-square velocity components of turbulent fluctuations.
u_*	14	Shear velocity.
v'_{dn}	13	Root-mean-square value of the downward part of $\bar{v}'$.
v'_{up}	13	Root-mean-square value of the upward part of $\bar{v}'$.

Symbol	Where introduced	Meaning
V	I 5	Fall velocity of suspended solids. Effective fall velocity of heterogeneous solids $= pV_p$.
$\tan \alpha$	4	‡Coefficient of solid friction $= T/P$.
η	10	Absolute viscosity of fluid.
θ	9	‡Dimensionless shear stress $= \frac{\tau}{(\sigma-\rho)gD}$.
λ	10	†Linear concentration $= \frac{\text{mean } D \text{ of solids}}{\text{mean free distance between solids}}$.
ν	10	Kinematic viscosity of fluid.
ρ	4	Density of fluid.
σ	4	Density of solids.
τ	5	†Mean boundary shear stress.
Ω	5	†Stream power per unit length of whole stream $= \rho g Q S$.
ω	I 5	†Stream power per unit boundary area $= \tau \bar{u}$.
b	4	Subscript pertaining to bedload.
c	7	Subscript pertaining to a moving boundary.
0		Subscript pertaining to conditions within stationary bed.
p	17	Subscript pertaining to the grain size present in proportion p.
s	4	Subscript pertaining to suspended load.
x	9	Subscript pertaining to critical value.
A, a, n, n'		Casual symbols confined to isolated contexts and denoting dimensionless parameters.
E, F, R, t, t_h		Other casual symbols confined to isolated contexts.

AN APPROACH TO THE SEDIMENT TRANSPORT PROBLEM FROM GENERAL PHYSICS

By R. A. Bagnold

INTRODUCTION

During the present century innumerable flume experiments have been done, and a multitude of theories have been published in attempts to relate the rate of sediment transport by a stream of water to the strength of the water flow. Nevertheless, as is clear from the literature, no agreement has yet been reached upon the flow quantity—discharge, mean velocity, tractive force, or rate of energy dissipation—to which the sediment transport rate should be related.

Consequently there is as yet no agreement on method of plotting measured transport rates against the transporting flow; for this reason little serious attempt has been made to correlate the results of laboratory experiments, either between themselves or with field data, or to discriminate between diverging theories by this means.

Indeed, the outlook is obscured by the very number of published theories. For example, the engineer research student, encouraged by degree thesis requirements to advance a new theory rather than to verify existing concepts, is able to find somewhere in the literature, and to quote, support for an assumption which best suits his argument.

The root cause of this unfortunate proliferation and diversity of ideas is evidently the absence of any sound and indisputable quantitative basis of reasoning compatible both with the facts and with the laws of nature and, therefore, commonly acceptable. Consensus of opinion, which varies from decade to decade, is no satisfactory substitute.

In most if not all other fields of modern technology such a general basis of reasoning has been supplied by the parent natural science, in the form of accepted relationships between quantities which are in some degree idealized. The technologist has merely to find by experiment how to adapt it to real measured quantities.

No established branch of physics has, however, interested itself in two-phase (fluid-solid) flow, which is involved in sediment transport. For the fluid-dynamicist has been reluctant to tackle its special problems until he has mastered the problems of fluid flow, and of fluid turbulence in particular, and can explain them quantitatively in terms of established natural laws.

Therefore, the hydraulic engineer, concerned with specific practical problems rather than with general scientific explanations of natural processes, solves his problems by empirical reasoning from past experience of like conditions. Thus different working formulae are found, each an approximation to the truth over a different limited range of conditions, within the man-made bounds of professional practice.

Attempts to weld these formulae together into a general empirical relationship, applicable under all conditions, have failed. This is to be expected because (*a*) reasoning from the particular to the general presents obvious difficulties, and (*b*) the test of success has been immediate applicability to specific practical problems rather than generality of agreement with the facts.

The following is an attempt made from the opposite direction, from the basis of reasoning deducible from the principles of physics. The measure of success is to be tested, not by immediate practical applicability, but by the extent of the range of conditions, practical or otherwise, over which it is found reasonably true. By "reasonably true" I mean that discrepancies are capable of rational explanation such as uncertainties of measurement by conventional methods.

The theory makes no pretense of being complete. Moreover, some conclusions run counter to conventional ideas. Nevertheless, the measure of agreement with the generality of fact over a very wide range of conditions suggests the likelihood that the general framework is sound in principle.

A theory is of doubtful value unless demonstrated to fit the facts. It has been necessary, therefore, to devote considerable space to the assembly and discussion of as many relevant facts as possible, so that the reader may judge the theory for himself. Such a pres-

entation of the facts, in the form of experimental plots and of tabulated river data, also serve the useful purpose of bringing to light the deficiencies in the experimental coverage.

The uncertainties about turbulence effects—such as those of boundary roughness, form drag, and sediment transport—on the flow resistance have been avoided by the simple expedient of treating both the mean flow velocity and the tractive force as independent, or given, variables. This seems wholly justifiable since the objective is to predict the transport of solids by the fluid flow and not to attempt to predict fluid flow itself, which lies within the proper province of the hydraulic engineer.

A number of theoretical aspects have already been discussed in a previous paper (Bagnold, 1956), to which frequent reference is made in this paper. However, by confining the conditions to those of transport by the open gravity flow of a liquid I have been able to make the previous theory considerably simpler and more directly applicable. Certain of the former tentative conclusions have, moreover, been modified.

Since the terms and symbols standardized in hydraulic textbooks are inadequate to deal with the transport of solids, the well-known shortage of suitable symbols has necessitated some revision of their conventional use.

Finally, in presenting any general theory about sediment transport some embarrassment arises from the great number of existing theories which have appeared during the present century in widely scattered publications. So many aspects have been discussed from so many viewpoints that it is doubtful whether any one person has read them all, let alone digested them sufficiently to appreciate all the implications of each. It is likely, therefore, that some of the notions here embodied have already been suggested by previous authors. My apologies are extended to any authors to whose work I have unwittingly omitted reference. At the same time it should be borne in mind that if the objective is a genuine quest for the truth it is immaterial whether the truth is new or old.

GENERAL CONSIDERATIONS

ESSENTIAL FEATURES OF GRANULAR FLOW

The bulk movement, or "flow," of granular solids occurs in a wide range of phenomena, from the mainly fluid-impelled transport of solids, naturally by wind and by water streams and industrially through closed pipes, to the spontaneous flow of supersaturated soils, and finally to simple granular avalanching or pouring in which the impulsion or traction is by the direct action of gravity on solids alone, unaided by any fluid traction.

The distinctive character of this class of phenomena is defined by the following essential features:

1. The motion is a shearing motion wherein successive layers of solids are sheared over one another.
2. An impelling or tractive force, applied in the direction of motion, is necessary to maintain the motion.
3. The array of solids is immersed in some pervading fluid, either a liquid or a gas, and this fluid also is under shear.
4. The solids are heavier than the fluid, and are therefore pulled downward toward a lower boundary or bed.
5. In steady continuing motion the forces acting on every layer of solids must be in statistical equilibrium.

IMPLICATION: THE EXISTENCE OF AN UPWARD SUPPORTING STRESS

Any general shearing of an array of solid grains requires some degree of dilation or dispersion of the array, in order to allow sufficient freedom for the shearing to take place. This was strikingly demonstrated by Reynolds (1885), who showed that when a mass of loose grains at rest is prevented from dilating it behaves as a rigid undeformable body.

When the solids are sheared over a gravity bed the dispersion must necessarily be upward, against the normal component of the gravity force. To maintain such shear thus requires the maintained exertion of an upward supporting stress of some kind on every granular shear layer.

Whatever may be the degree of upward dispersion, equilibrium demands that across any shear plane the magnitude of this supporting stress, of whatever kind, must be equal to the immersed (excess) weight of the solids present above that plane.

The above points are indisputable. The existence of an upward supporting stress equal to the immersed weight of the superimposed solids and the mechanisms by which it is maintained emerge as the nub of the problem. This important aspect has often been neglected because the traditional approach has been largely kinematic.

In a problem such as the present one, which concerns the effects of a density difference, any kinematic approach seems to be inherently self-defeating. For by eliminating the concepts of mass and force, the effects of forces due to density differences are removed from consideration. The problem immediately becomes indeterminate, because any determinate relationship exists only by virtue of these effects. If there is no density difference, the transport rate then depends only on the availability of transportable material.

The introduction of the density difference indirectly, as implicit in the fall velocity of a representative solid, is clearly inadequate, for this approach fails to introduce the quantity of such solids transported. Since the quantity is the core of the problem, the problem remains as indeterminate as before.

There can therefore be no alternative to facing the following questions of dynamics: By what mechanism can the necessary upward supporting stresses be transmitted from the bed to the dispersed solids? How are these stresses maintained? And what determines the magnitude of the stresses?

The first question can be answered at once. There are only two possible mechanisms by which mechanical forces can be transmitted:

1. By the transfer of momentum from solid to solid by continuous or intermittent contact. For example, whether I hold a ball in my hand, or repeatedly throw it up and catch it, or repeatedly pick it up and drop it, or throw it away so it bounces repeatedly over the ground, the weight of the ball is supported only by solid contact.[1] When the ball is apparently unsupported it is in fact supported by the impulse of a previous contact. And over a period of time the weight of the ball is precisely equal to the mean upward flux of momentum per unit of time, irrespectively of what I do with the ball.
2. By the transfer of momentum from one mass of fluid to another and thence to the otherwise unsupported solid. For example, an overweighted (nonbuoyant) balloon can maintain its height above the ground if it happens to drift from one upward air current to another. If this were to continue indefinitely the excess weight of the balloon would be found to be precisely equal to the mean upward flux of fluid momentum transferred to it.[2] Continued support by this mechanism requires the continued maintenance of upward fluid currents whose effects exceed those of corresponding downward currents. The implications of this requirement are discussed later.

The second question also can be answered at once. The support mechanism is maintained by the shearing motion, which in turn is maintained by the applied tractive force. The solid-transmitted stress arises from the shearing of the solids over one another, for this stress can be shown to exist in the absence of any fluid at all—when a mass of solids is sheared by allowing it to avalanche or pour in an evacuated vessel. The fluid-transmitted stress must clearly arise from the shearing of the fluid, for it is this which maintains the necessary internal turbulent motion.

The answer to the third question, as to the magnitude of the supporting stresses and therefore of the immersed weight of solids in transit over unit bed area, is given later in this paper.

RESTRICTIONS OF CONDITIONS TO BE CONSIDERED

The application of dynamics to any problem requires at the outset a clear definition of the system to be considered. For simplicity the conditions are restricted to the following:

1. Steady open-channel liquid flow by gravity.
2. Unlimited availability of transportable solids.
3. The concentration of transported solids, by immersed weight, is sufficiently small that the contribution of the tangential gravity pull on the solids to the applied tractive stress can be neglected.
4. The system considered is defined as statistically steady and as representative not of conditions at a single crosssection but of average conditions along a length of channel sufficient to include all repetitive irregularities of slope, crosssection, and boundary.

Restriction 1 excludes transport by atmospheric wind because the motive power of the wind is less readily definable than that of a liquid stream of finite depth. Restrictions 1 and 2 together exclude the industrial transport of solids through closed pipes, wherein a granular bed is nonexistent and the impulsion is by a pressure gradient instead of by gravity. Restriction 3 is not essential; it merely avoids complications. Restriction 4 is essential, for it permits energy considerations to be precise.

These restrictions leave the reasoning applicable to nearly all the conditions likely to prevail both in laboratory flumes (whether the flow is turbulent or laminar) and in most natural rivers.

BEDLOAD AND SUSPENDED LOAD AND THE WORK RATES OF THEIR TRANSPORT

DEFINITIONS

The excess weight of solids in transit over unit bed area must be supported by one or the other of the two before-mentioned momentum transfer mechanisms. If shear turbulence exists, many individual solids are likely to be supported partly by one mechanism and partly by the other. We can, however, without any loss of generality treat a large number of solids statistically, and divide their excess weight into two discrete parts.

[1] Although there may be local and transient exchanges of momentum between the ball and an immersing fluid whose internal motion, if any, is isotropic, the normal components of these cancel out. The fluid plays no overall part in the support, which is transmitted solely by solid contact.

[2] Continued support in this way would be impossible were the random internal atmospheric motion to be isotropic. An anisotropic fluid motion is required, such as required, such as that of shear turbulence.

208-578—66——2

If the dry mass of the solids is m and their density σ, the immersed weight is $m'g=\frac{\sigma-\rho}{\sigma}mg$, where ρ is the density of the fluid. We can divide m' into two parts m_b' and m_s' defined as follows:

The bedload m_b' is that part of the load which is supported wholly by a solid-transmitted stress $m_b'g$, and the suspended load m_s' is that part which is supported by a fluid-transmitted stress $m_s'g$.

No experimental means having yet been found by which to measure separately the magnitude of either m_b' or m_s', or even to measure the total load m', these quantities have attracted little attention. They are nevertheless real and relevant.

Similarly, no experimental means have been found by which to measure the mean transport velocities U_b and $\bar{U}_s$ of the solids.[3]

However, the total transport rate is directly measurable under laboratory conditions. Denoting the conventional transport rate—that is, the dry mass passing in unit time over unit width of the bed—by the symbol j, evidently

$$j=m\bar{U}=m_b\bar{U}_b+m_s\bar{U}_s \qquad (1)$$

But since we are concerned with actual dynamic stresses the transport rate for dry mass is clearly inappropriate and should be replaced by the transport rate for immersed weight. Denoting this by the symbol i,

$$i=\frac{\sigma-\rho}{\sigma}gm\bar{U}=i_b+i_s=m_b'g\bar{U}_b+m_s'g\bar{U}_s \qquad (2)$$

TRANSPORT WORK RATES

It can be seen that the dynamic transport rates j_b and i_s have the dimensions and quality of work rates, being the products of weight force per unit bed area times velocity. As they stand, however, they are not in fact work rates, for the stress is not in the same direction as the velocity of its action.

The dynamic transport rates become actual work rates when multiplied by notional conversion factors A_b and A_s, each defined as the ratio

$$\frac{\text{tractive stress needed to maintain transport of the load}}{\text{normal stress due to immersed weight of the load}}$$

Both A_b and A_s must necessarily have finite values. For if either were zero the fundamental principle underlying the so-called second law of thermodynamics would be violated; perpetual motion would be possible. In fact, no form of continuing material transport can possibly take place under the influence of a continuing transverse pull on the material without accompanying energy dissipation in resisting the transverse pull. Some theories have overlooked this.

PRINCIPLE OF SOLID FRICTION AND BEDLOAD WORK RATE

Although both solid and fluid friction dissipate energy, they differ greatly in character. Solid friction, treated in elementary physics, is omitted from hydraulic textbooks.

When two solid bodies in contact under a normal force P are sheared over one another, a tangential shear force T is required to maintain relative motion (fig. 1A). The coefficient of solid friction is defined as the ratio T/P. This ratio is found to be a constant for the materials of the contact surfaces. Unlike fluid friction, solid friction in general is independent of the relative velocity of shear so long as the energy dissipation as heat is insufficient to change the character of the contact surfaces. "Stick-slip," as between violin bow and string, is exceptional. With the same proviso, the ratio T/P is independent of the absolute values of T and P.

The coefficient of solid friction is most easily measured by resting one body upon the other and increasing the angle α of inclination of the shear plane until shearing begins by gravity (fig. 1B). Then since $T=Mg\sin\alpha$, and $P=Mg\cos\alpha$, the coefficient $T/P=\tan\alpha$.

The limiting static coefficient for a mass of cohesionless granular solids is measurable in the same way, from the limiting angle of repose at which the surface of the mass stands without shearing. The angle for most sands is approximately 33°, for which $\tan\alpha=0.63$.

The dynamic condition when the mass of grains is under continuing shear, with mutual jostling motions in all directions, was investigated experimentally (Bagnold, 1954), and the application of the results to bedload transport was discussed (Bagnold, 1956).

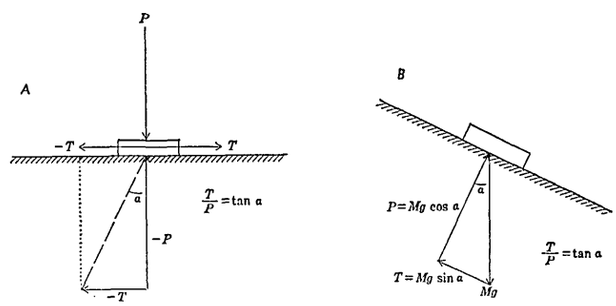

FIGURE 1.—Relation of normal force or stress to tangential force or stress between solids in moving contact.

[3] Velocities of solids in the direction of transport are denoted by $\bar{U}$ and velocities of the fluid by $\bar{u}$. The conventional symbol G for the mass transport rate is unsatisfactory, since it may ambiguously refer to the whole transport or to that per unit width. Small i and j are here used for transport rates per unit width, leaving I and J for the transport rates over the whole width of the bed.

For the moment it is sufficient to state that the dynamic friction coefficient or stress ratio T/P across shear planes of an array of solid grains is of the same order as the static coefficient, not only when the grains are closely packed but also when they are considerably dispersed. The above work established the existence of a direct frictional opposition to the impulsion of a bedload, the opposing stress, in the direction of motion, being proportional to the excess weight of the load.

The factor A_b immediately becomes the friction coefficient tan α, which is a measurable parameter. Substituting the immersed load stress $m_b'g$ for P, the opposing stress in the direction of motion is $m_b'g$ tan α, and

$$\text{bedload work rate}=m_b'g\overline{U}_b \tan\alpha=i_b\tan\alpha \quad (3)$$

Here the angle α is associated with the average angle of encounter between individual grains, and tan α is the ratio of the tangential to the normal components of grain momentum resulting from the encounters.

SUSPENDED-LOAD WORK RATE

The suspended-load work rate can be inferred simply and indisputably. The suspended solids are falling relative to the fluid at their mean fall velocity V. But the center of gravity of the suspension as a whole does not fall relative to the bed. Hence the fluid must be lifting the solids at the velocity V. The rate of lifting work done by the shear turbulence of the fluid must therefore be

$$\text{suspended-load work rate}=m_s'gV=i_s\frac{V}{\overline{U}_s} \quad (4)$$

The factor $A_s=V/\overline{U}_s$ may be regarded as the counterpart of tan α. The fluid shear turbulence is in effect pushing the suspended load up a notional frictionless incline $V/\overline{U}_s$.

TRANSPORT WORK RATES AND AVAILABLE POWER; THE GENERAL SEDIMENT-TRANSPORT RELATIONSHIP

THE GENERAL POWER EQUATION

When any kind of continuing work is being steadily done the principle of energy conservation can be expressed in terms of the time rates of energy input to, and output from, a specified system by the equation

rate of doing work=available power−unutilized power

or in an equivalent alternative form

$$\text{rate of doing work}=\text{available power}\times\text{efficiency} \quad (5)$$

This basic equation has long been familiar to engineers in other fields—such as mechanical, hydromechanical, and electrical—concerned with working machines and with power transmission. It has attracted but little attention, however, in the field of channel hydraulics, and no conventional symbol has been allotted to the quantity power.

The power equation appears first to have been applied to sediment transport by Rubey (1933) and later by Velikanov (1955). It was again suggested by Knapp (1941), and was later introduced by me in a paper (Bagnold, 1956) wherein the flowing fluid was regarded as a transporting machine. But none of these ideas have been followed up by taking the logical step of plotting experimental transport rates against stream power.

AVAILABLE STREAM POWER

The available power supply, or time rate of energy supply, to unit length of a stream is clearly the time rate of liberation in kinetic form of the liquid's potential energy as it descends the gravity slope S. Denoting this power by Ω,

$$\Omega=\rho gQS$$

where Q is the whole discharge of the stream.

The mean available power supply to the column of fluid over unit bed area, to be denoted by ω, is therefore

$$\omega=\frac{\Omega}{\text{flow width}}=\frac{\rho gQS}{\text{flow width}}=\rho gdS\bar{u}=\tau\bar{u} \quad (6)$$

The kinetic energy ω liberated in unit time and subsequently dissipated as heat must not be confused with the energy stored within the fluid at any given instant. The liberated energy is as little related to the stored energy as is the inflow and outflow of water through a reservoir related to the quantity of water stored in the reservoir.

Confusion is sometimes caused by the seeming paradox that at a given tractive or motive force an increase of resistance has the effect of reducing the power dissipation even though the extra resistance element itself introduces an added element of power dissipation. The reason is immediately clear from the electrical analogy. The electric power dissipated at a given voltage E is $I^2R=E^2/R$. Hence if we increase the resistance R to $R+R'$, the power dissipation is decreased in the ratio $R/(R+R')$ even though the extra series resistance R' itself dissipates a new power element I^2R'.

Uncertainties as to the precise energy state existing at any point or cross section have led many to prefer momentum to energy considerations. However, in statistically steady channel flow no such uncertainties arise as to the time rate of energy supply and dissipa-

tion, provided the system considered is defined as representative of the flow along a length of channel sufficient to include all repetitive irregularities of slope, cross section, and boundary, and the consequent periodic energy transformations.

The available power and the transport work rates, regarded as so defined, have precise average values along a channel although their values at any specific cross section may be imprecise.

The available power has the same dimensions and quality as the rate of transporting work done. And since the dynamic transport rate i of the solids also has these dimensions and quality, there can be no reasonable doubt that the transport rate is related primarily to the available power, as in all other modes of transport.

THE GENERAL TRANSPORT RELATIONSHIP IN OUTLINE FORM

The available power ω constitutes the single common supply of energy to both the transport mechanisms. Applying equations 3 and 5 for bedload transport, we have

$$i_b \tan \alpha = e_b \omega \text{ or } i_b = \frac{e_b \omega}{\tan \alpha} \tag{7}$$

where e_b is the appropriate efficiency, necessarily less than unity.

The work power $e_b\omega$ is dissipated directly into heat, in the process of solid friction. It has gone. Hence, for turbulent fluid flow, the power available to do the work of supporting a suspended load is $\omega(1-e_b)$.

Applying equations 4 and 5 for suspended-load transport, we have therefore

$$i_s \frac{V}{\overline{U}_s} = e_s \omega (1-e_b) \text{ or } i_s = \omega \frac{e_s \overline{U}_s}{V} (1-e_b) \tag{8}$$

Adding equations 7 and 8 the expression for the whole transport rate i is

$$i = i_b + i_s = \omega \left(\frac{e_b}{\tan \alpha} + \frac{e_s \overline{U}_s}{V} (1-e_b) \right) \tag{9}$$

The derivation of this general outline relationship seems to me straightforward and logical. It involves neither assumption nor approximation, and it is applicable both to turbulent and to laminar fluid flow.

In laminar flow the second term disappears, for suspension as here defined cannot occur, all the solid material being transported as bedload.

We have now to infer the values of the four parameters e_b, tan α, e_s, and $\overline{U}_s$.

By an approximation which should be reasonably close for most purposes, we can at once reduce the number of parameters to three. For since the travel of the suspended solids is unopposed, they can be assumed to travel at the same velocity as the fluid surrounding them. The error introduced by substituting the mean velocity $\overline{u}$ of the fluid for the mean velocity $\overline{U}_s$ of the suspended solids lies only in the differing distributions of fluid and solid discharges with distance from the bed. The possible small error introduced into what follows by making this substitution should be borne in mind.

BEDLOAD TRANSPORT EFFICIENCY e_b AT HIGH TRANSPORT STAGES

CONCEPT OF A MOVING FLOW BOUNDARY

The conventional kinematic definition of a boundary to shear flow is a surface at which the flow velocity is zero relative to the boundary. In channel hydraulics the boundary is assumed axiomatically to be fixed relative to the ground. An equally valid, and more general, dynamic definition of a boundary to shear flow is a surface, or a zone of finite thickness, at or within which the fluid shear stress is reduced to zero by transfer to another medium. The boundary medium may or may not be fixed relative to the ground.

At the threshold of motion of the solids both e_b and e_s are evidently zero. The solids are all stationary on the bed. So the flow of the fluid is relative to a boundary which is stationary relative to the ground.

As the available power is increased, however, more and more solids move over the bed as bedload, and consequently more and more of the boundary shear stress is applied to the stationary bed indirectly in the form of the solid-transmitted frictional stress T via the moving bedload solids.

In this transitional range of flow stage, therefore, the fluid flow is relative to a boundary which is partly moving and partly stationary. Both the internal structure of the flow and the velocity distribution are likely to be complex.

As the bedload increases, however, a critical stage must be reached at which so great a number of bedload solids cover the stationary surface as a moving layer that in effect this layer occludes the stationary surface from the fluid flow above it.

At and beyond this critical stage, therefore, the fluid flow is wholly relative to a boundary which is itself moving relative to the ground. The fluid shear stress τ at this moving boundary may be regarded as disappearing, the fluid-transmitted shear stress being converted progressively through the thickness of the layer into the solid-transmitted shear stress T.[4]

[4] Experiment (Bagnold, 1956, p. 242) has indicated that at granular concentrations prevailing immediately over a stationary grain bed at the higher flow stages less than 1 percent of the shear stress is maintained by the intergranular fluid, the remainder being maintained by the solid-transmitted stress T.

As a first step toward arriving at the efficiency e_b under these conditions, let the moving granular flow boundary be replaced by a continuous carpet. The carpet is supposed in contact with the stationary bed, and has a varying weight $m'g$ proportional to the applied shear stress. The motion of the carpet is opposed by solid friction at its underface.

The fluid flow above the carpet applies a fluid shear stress τ to it. Provided the carpet is thin compared to the depth of the flow, the resisting shear stress T at its underface is equal to τ above it. The conditions are as sketched in figure 2*A*.

The problem is now as follows: If the flow is of given depth and has a given mean flow velocity $\bar{u}$ relative to the ground, what is the maximum limiting rate at which the flow can do work in transporting its boundary along the ground?

The mean velocity of the flow relative to its own boundary is $\bar{u}-U_c$, where U_c is the transport velocity of the boundary.

For generality, let the flow law be

$$\tau=a(\bar{u}-U_c)^n$$

where n is 2 for fully turbulent flow and 1 for laminar flow.

If the thickness of the carpet boundary is negligible compared to the flow depth, $T=\tau$ and the rate of transporting work done is

$$TU_c=\tau U_c=aU_c(\bar{u}-U_c)^n$$

This function has two zero values, when U_c equals zero and $\bar{u}$, and one maximum value, when $U_c=\bar{u}/(1+n)$.

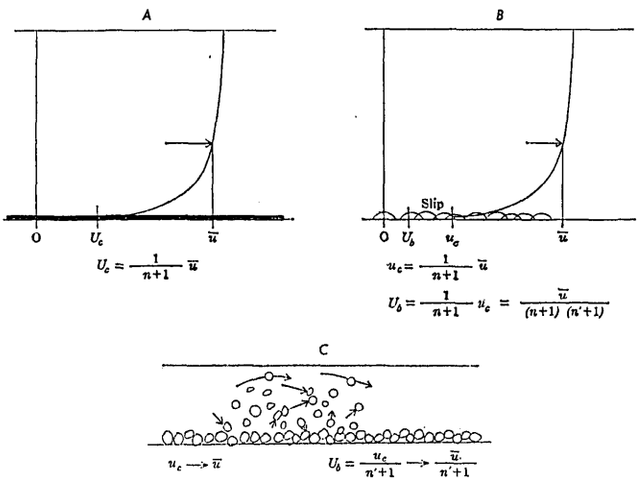

FIGURE 2.—Flow relative to moving boundaries. *A*, Flow relative to a moving carpet. *B*, Flow relative to a moving granular boundary of negligible thickness. *C*, Effect of inadequate flow depth and appreciable boundary thickness.

Hence the maximum transport efficiency is as follows:

$$e_c=\frac{TU_c}{\tau\bar{u}}=\frac{1}{(1+n)} \tag{10}$$

which is one-third for fully turbulent flow and one-half for laminar flow.

These results are unaffected by the replacement of the single carpet layer by a number of superimposed carpet layers in solid contact with one another, provided the total thickness is negligible in comparison to the flow depth. Let the superimposed layers each have some unspecified thickness t proportional to the number of real granular solids each represents. The shear force on any layer t_h, moving at a velocity U_h, is $\tau\frac{t_h}{\sum t}$, and the work rate of moving the layer is $\tau\frac{t_hU_h}{\sum t}$. The whole work rate is therefore

$$\tau\frac{\sum(t_hU_h)}{\sum t}=\tau\overline{U}$$

As a second step consider the essential difference of condition between that of a continuous-carpet flow boundary and that of a boundary consisting of dispersed solids. This difference lies in the fact that whereas the fluid shear stress τ is applied directly to a continuous boundary, its application to a dispersed granular boundary necessarily involves relative motion between the constituent grains and the fluid in their immediate neighborhood. Hence the transport velocity U_b of the boundary material is less than the velocity $\bar{u}_c$ of the boundary it constitutes (fig. 2*B*).

The transfer of stress from fluid to solids involves a local dissipation of energy. This introduces a further efficiency factor $e_g=U_b/\bar{u}_c$, so that $e_b=e_c\cdot e_g$, where, as we have seen, e_c is one-third for fully turbulent flow.

The limiting value of e_g follows from the same line of reasoning as before, applied to the local flow in the neighborhood of the bedload grains rather than to the whole flow. Consider this time a single representative bedload grain. Under steady average conditions the fluid force F urging it along is in equilibrium with an equal mean frictional force applied to it intermittently by the bed.

The force F varies as $(u_c-U_b)^{n'}$ where n' varies between 1 and 2 according to the local Reynolds number $\mathbf{R}=(u_c-U_b)D/\nu$, being 1 in the ultimate Stokes law region and 2 for large grains. The work rate $U_b(u_c-U_b)^{n'}$ has a limiting value when $U_b/u_c=e_g=1/(n'+1)$.

The exponent n' for a given grain size D and a given $\mathbf{R}$, that is, for a given slip velocity u_c-U_b, can be obtained from the slope of the experimental log curve of

drag coefficient versus **R**. If the slope at any point on the curve is a, then $n'=2-a$. Since

$$u_c=(u_c-U_b)\frac{n'+1}{n'} \text{ and } u_c=\frac{1}{3}\bar{u}$$

for fully turbulent flow, values of e_g and e_b can be found corresponding to a range of arbitrary values of the mean flow velocity $\bar{u}$. These efficiency values are shown in figure 3 for various grain sizes D (quartz-density grains in water). The bedload efficiency e_b should range from 0.11 for large grains and large flow velocities to 0.15 for very fine grains and low flow velocities.

The whole rate of energy expenditure in transporting the bedload consists of the work rate $e_b\omega+e_c\cdot e_g\omega$ plus the ineffective power dissipation $e_c\omega(1-e_g)$ involved in the local transfer of stress from fluid to solids. It might at first sight be thought that in the transport of large grains since this latter dissipation takes place through the creation of wake eddies some of it may be available to maintain the turbulent suspension of smaller grains. But, as later becomes apparent, this kind of turbulent eddy is unlikely to possess the essential quality of boundary shear turbulence necessary to maintain a suspension. Therefore, the overall power loss attributable to the bedload transport is $e_c\omega=\frac{1}{3}\omega$, so that only $\frac{2}{3}\omega$ remains available to maintain a suspended load.

CRITICAL STAGE BEYOND WHICH THE BEDLOAD EFFICIENCY e_b SHOULD BE PREDICTABLE

The foregoing argument is restricted to conditions in which the moving bedload solids are sufficiently numerous to interpose an effective flow boundary between the free fluid flow above and the stationary bed below. By the foregoing dynamic definition of a flow boundary the above condition is fulfilled when virtually the whole applied fluid stress is transferred to the moving bedload solids.

The critical bedload stage appears therefore to be definable by a critical value of the bed stress τ.

A rough estimate of this critical value can be obtained as follows. The topmost stationary grain layer of the bed effectively occludes the fluid flow above it from the stationary layer immediately beneath it. Hence

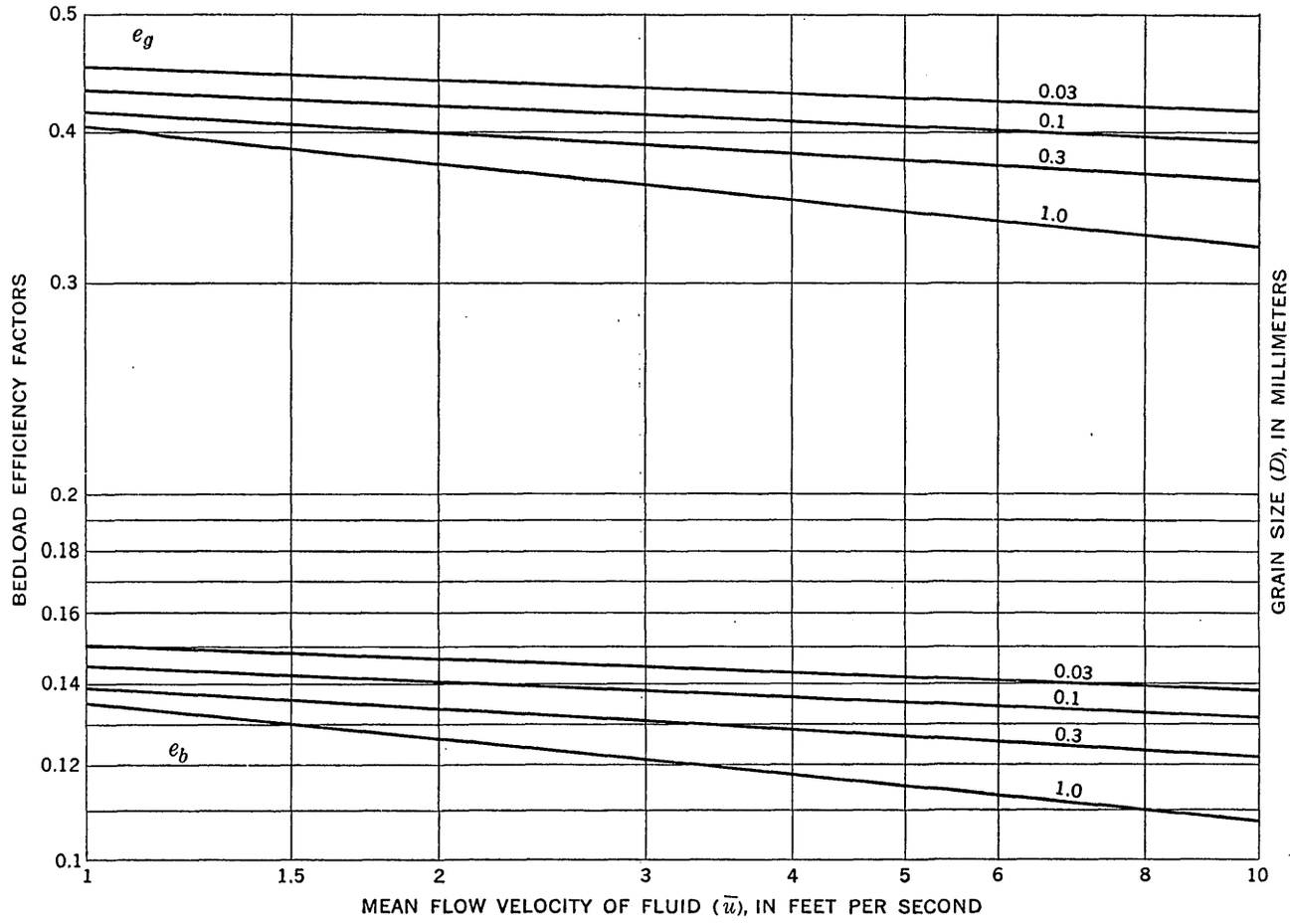

FIGURE 3.—Values of theoretical bedload efficiency factors, in terms of mean flow velocity, for quartz-density solids in an adequate depth of fully turbulent water.

this occlusion can be expected to persist if the whole topmost layer is set in motion as bedload over the layer beneath, which has now become the topmost stationary layer.

The immersed weight of the original topmost layer, which is now in motion, is $(\sigma-\rho)gD\cdot C_0$ where D is the mean grain size, and C_0 is the static volume concentration, that is, (1—porosity), whose average value may be put at 0.6 to 0.7.

The bed shear stress τ required to maintain the motion of this load is

$$\tau=(\sigma-\rho)gDC_0 \tan \alpha$$

Introducing θ as the dimensionless bed shear stress $\tau/(\sigma-\rho)gD$, the critical stage should occur when, approximately,

$$\theta_x=C_0 \tan \alpha \qquad (11)$$

From experiment, tan α appears to vary according to the conditions of shear from 0.375 to 0.75 owing to the variation of fluid-viscosity effects with variation of grain size and mass. The estimated range of θ_x from about 0.5 for grains smaller than 0.3 mm to about 0.25 for grains larger than 2.0 mm is sketched in figure 4. This range is derived from a more basic relationship, figure 5, introduced under the later heading "Variation of the dynamic bedload friction coefficient tan α."

It should be realized that any direct manifestation of this critical stage concerning the bedload by a change in the trend of experimental plots of total transport rate against the power may, for fine grains, be masked by a more pronounced change resulting from the attainment of a corresponding critical stage at which the suspended load becomes fully developed.

However, as suggested previously (Bagnold, 1956, p. 256), the critical bedload stage θ_x is likely to be broadly associated with the value of θ at which bed features disappear or at any rate cease to create appreciable form drag. The experimental evidence (figs. 9–13) shows the correspondence to be moderate.

This evidence is somewhat indefinite. The change from large-scale dunes to flat beds occurs gradually over a considerable range of stage, and different observers tend to discriminate differently. The experimental scatter adds to the uncertainty. As can be seen, some reported dunes widely overlap with reported flat beds.

More precise experimental work is needed before a satisfactory criterion is found by which to predict for a given sediment the critical stage at which the change of end occurs in the transport-rate plots.

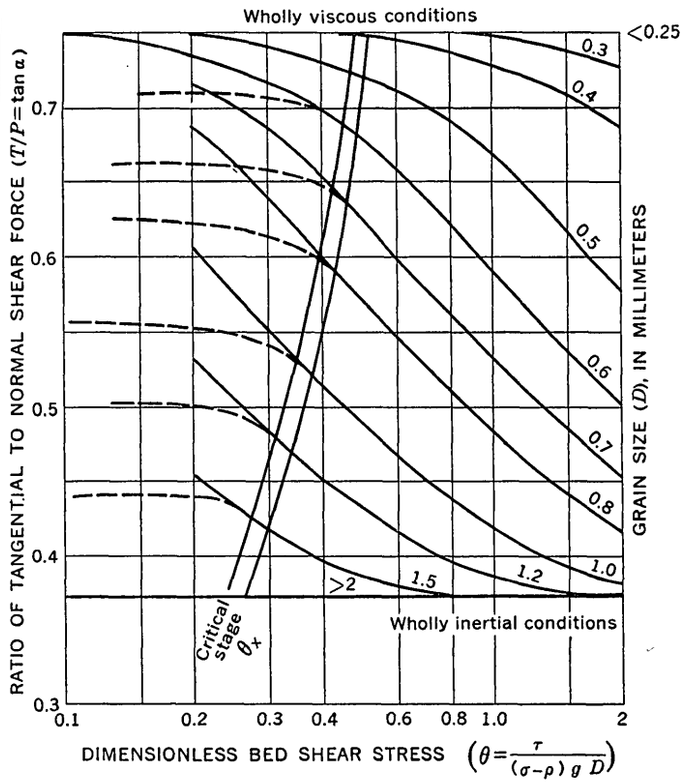

FIGURE 4.—Values of the solid-friction coefficient tan α in terms of the bed-stress criterion $\theta=\tau/(\sigma-\rho)gD$ for quartz-density solids of various sizes in water, derived from figure 5, and the predicted critical values of θ beyond which the theory should be applicable.

EFFECT OF INADEQUATE FLOW DEPTH ON THE VALUE OF e_b

In a previous subsection of this paper the evaluation of the bedload efficiency factor e_c as being $1/(n+1)=1/3$ for fully turbulent flow depended on the assumption that the thickness of the conceptual moving carpet could be neglected in comparison to the flow depth.

As the flow depth is progressively reduced, a point must clearly be reached at which this assumption becomes invalid. Consider the extreme case when the water surface coincides with the height reached by the saltating solids (fig. 2*C*). The fluid shear stress is now transferred to the solids throughout the flow. The moving-carpet concept entirely breaks down, and e_c approaches unity. The bedload efficiency e_b is nearly three times greater, and approaches e_s in value.

At a given power, therefore, the transport rate of bedload would be three times greater than the rate to be expected at greater flow depths.

This immediately raises the question, what is the effective thickness of the bedload zone at high stages when the number of moving solids is equivalent to the number in several grain layers of the bed? This question is of some importance; for if flume experiments are to be representative of river flow the experimental flow

depths must exceed some multiple, say 10, of this thickness. Otherwise the experimental transport rates would be expected to be too large by an appreciable factor.

It appears that no reliable factual knowledge exists on this point. The conventional assumption that the bedload zone is but 2 to 3 grain diameters thick is based solely on visual observation of individual saltation paths at such very low stages close to the threshold of motion that the individual paths can be picked out.

At the higher stages this assumption is untenable on spatial considerations alone. The probability that the saltations will be interrupted by collisions between rising and falling grains becomes rapidly greater as the number of saltating grains increases.

Moreover, whatever may be the actual nature of the forces initiating a saltation, these forces, and with them the height attained, would be expected to increase approximately as the square of the flow velocity $\bar{u}$. And since the number of grains moving over unit bed area increases as the shear stress τ, the effective thickness of the bedload zone would be expected to increase as a function of the power omega. Hence, if the flow depth were inadequate, e_b would increase with increasing power instead of remaining virtually constant over the higher range of stages.

This consideration is directly relevant to a later discussion of the marked discrepancy between Gilbert's experimental transport-rate data, obtained at small flow depths of 0.1 to 0.3 feet and other comparable data obtained at flow depths several times greater. It is also directly relevant to the vexing problem of the proper allowance to be made for the effects of wall drag in laboratory flumes.

It would seem impossible to gage the height to which the bedload saltation rises at high stages of turbulent water flow, because of the presence of a concurrent suspended load. However, the saltation mechanism cannot depend on turbulence (unless we postulate two different mechanisms having identical effects), for saltation persists unchanged in appearance when the flow is made purely laminar. Much could therefore be learned about the effective thickness of the bedload zone at high stages by increasing the viscosity of the fluid till both turbulence and suspension disappear. A light machine oil of viscosity about 2 poise would seem suitable.

When a correction is made for the effect of increased viscous drag on the rising grain, I would not be surprised if the estimated thickness of the bedload zone in water at stages corresponding to θ values between say 0.5 and 2 was found to be as large as 20 to 50 grain diameters.

VARIATION OF THE DYNAMIC BEDLOAD FRICTION COEFFICIENT TAN α

The basic experiments discussed previously (Bagnold, 1954, 1956) showed that the dynamic friction coefficient $T/P = \tan \alpha$ varies over a factor of 2 according to the relative effects of grain inertia and fluid viscosity on the internal grain motions.

The grain stress ratio T/P may be regarded as the ratio of the tangential to the normal components of grain momentum associated with the impacts between grains as they are sheared over one another within the fluid.

The normal momentum component created at an impact between solids must necessarily be outward, tending to disperse one from another, as every billiard player knows. If the grains are assumed to be elastic, this normal component consists of two equal elements associated respectively with approach and rebound. In a viscous fluid all the rebound element may be transferred to the fluid during the time of passage of a grain to the next impact. But in a nonviscous fluid no such transfer takes place. Hence the effect of a change from viscous to inertial conditions is to double the normal momentum component. The tangential component on the other hand is not affected, since the mean forward motion of the grains remains the same, being determined by the imposed rate of shear. Hence the change from viscous to inertial conditions has the effect of doubling the dispersive grain stress P and therefore of halving the friction coefficient T/P.

Any change from viscous to inertial conditions of motion of either solids or fluids is definable by a criterion of the form of a Reynolds number. For solids the number was found to take the form

$$G = \frac{D}{\eta}\sqrt{\frac{\sigma T}{\lambda}} \qquad (12)$$

where η is the dynamic viscosity, σ is the density of the solids, T is the solid-transmitted shear stress, and λ is the linear spatial concentration defined by the ratio

$$\lambda = \frac{\text{mean diameter } D \text{ of solids}}{\text{mean free distance between solids}}$$

It can be seen that in its equivalent form

$$\frac{D}{\eta/\sigma}\sqrt{\frac{T}{\sigma\lambda}}$$

G is very closely analogous to the fluid Reynolds number

$$\frac{D}{\nu}\sqrt{\frac{\tau}{\rho}}$$

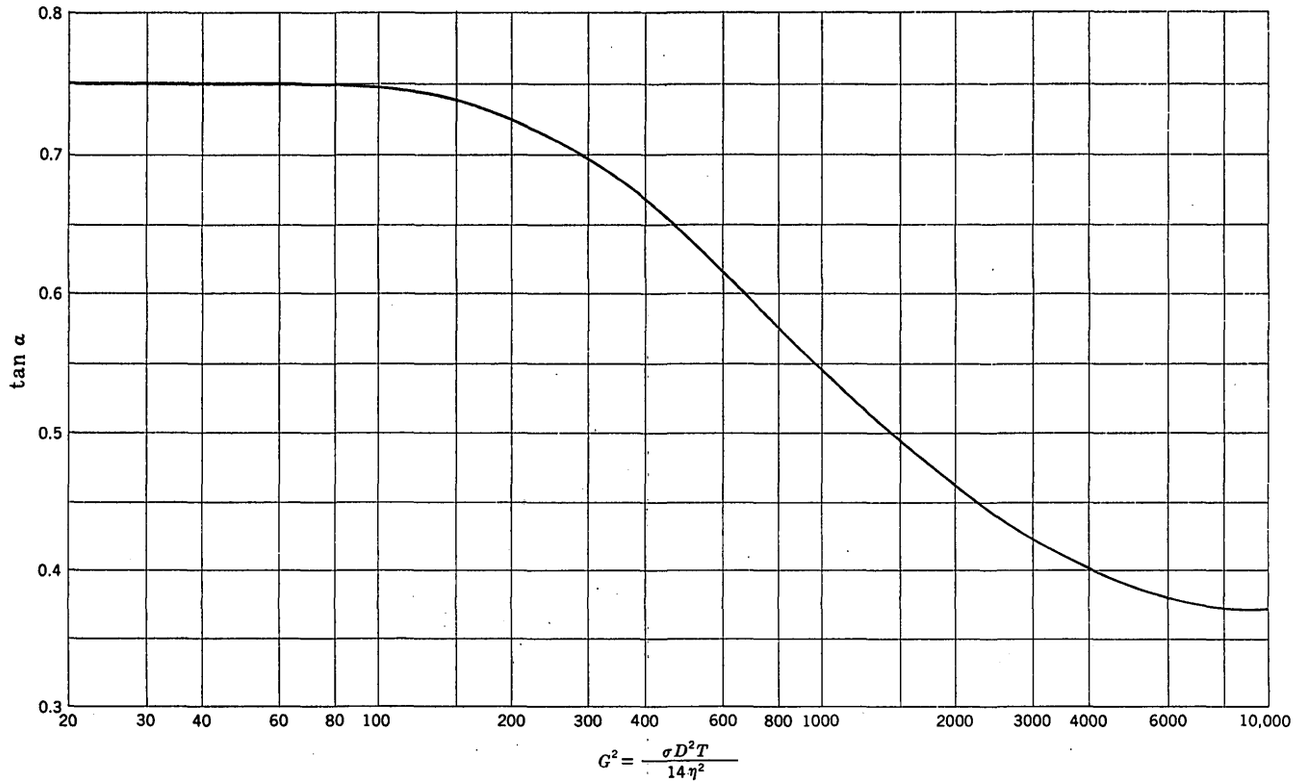

FIGURE 5.—Values of the solid-friction coefficient tan α in terms of the Reynolds-number criterion G for granular shear.

Experimentally, the change of conditions of motion was found to occur within a range of G between 10 and 90. The corresponding change in the numerical values of $T/P=\tan\alpha$ are shown graphically in figure 5. From this the values of tan α at and above the critical stage for bedload movement over a gravity bed can be calculated on the assumptions that (*a*) over the higher stages $T=\tau$ and (*b*) the concentration λ_0 at the bed surface remains constant at 14, which is the limiting concentration at which a sheared array of solid grains was found to cease to behave as a Newtonian fluid, and to begin to behave as a rheological "paste."

On these assumptions

$$G^2=\frac{\sigma D^2\tau}{14\eta^2}=\frac{\sigma D^3(\sigma-\rho)\theta}{14\eta^2} \tag{13}$$

where $\theta=\frac{\tau}{(\sigma-\rho)D}$ and τ is in engineers weight-force units and does not involve g.

The resulting values of tan α in terms of θ are shown by the family of identical curves in figure 4.

It should be noted that equation 13 is inapplicable to the lower transitional stages below the critical stage, because in equation 12 T is not equal to τ and λ is not constant. Both must dwindle to zero at the threshold of bedload motion. Grounds were given previously (Bagnold, 1956, p. 260) for assuming that over the transitional stage G may remain appreciably constant and thus make tan α constant as shown in figure 4.

Some support for these quantitative inferences is provided by the following:

1. Visible saltation—of quartz grains in water—as a manifestation of the effects of grain inertia has been reported (Durand, 1952) to fade out progressively as the grain size is reduced from 2 to 0.2 millimeter. As can be seen from figure 4 this is precisely the range of the change from wholly inertial to wholly viscous conditions.
2. According to the reasoning given previously (Bagnold, 1956, p. 254), instability at the bed-surface interface resulting in bed features, such as ripples, should occur only when the dynamic value of tan α within the moving bedload exceeds the static value tan α—that is, approximately 0.63—within the stationary bed. As can be seen from the broken curves in figure 4 this result should restrict the occurrence of spontaneous bed features, in water, to beds of mineral-density grains smaller than a size between 0.7 and 0.8 mm, in good agreement with observation.[5]

[5] Long flat scalelike features do occur on beds of much larger grains. But these features appear to be transient and to result from some disturbance which has caused a temporary local deposition—for example, a temporary excess of sediment fed to a noncirculating flume.

3. As reasoned on page 256 of the above paper, spontaneous features on beds of grains below the critical size should flatten out when the residual fluid-transmitted shear stress τ exerted directly on the stationary bed disappears—that is, when $\tau = T$ at the critical stage. The reader can judge for himself later how far this prediction is borne out experimentally.
4. Perhaps the strongest evidence is offered by the behavior of windblown sand. Here, owing to the relatively small value of the viscosity η, 1.2×10^{-4} poise instead of approximately 10^{-2}, all natural dune sands behave inertially ($G^2 > 8000$, fig. 5). We can, however, reduce the value of G^2 by reducing the grain size D in equation 13. The theory would predict that when G^2 is reduced—by giving appropriate experimental values to D and θ—to the critical value of approximately 530, for which $\tan\alpha = \tan\alpha_0 =$ the static value 0.63, conditions at the dry bed surface should become similar to those under a water stream. The typical ballistic pattern of wind ripples should then change to the very different water-stream pattern. Experiments in a wind tunnel confirmed this (Bagnold, 1956, p. 262 and pl. 2). The change took place abruptly, and at the predicted values of D and θ.

The original experiments, on the results of which figures 4 and 5 and equation 12 are based, were done on the shearing of artificial grains of zero excess density in water and other fluids, contained within the annular space between rotating drums (this being the only practicable way of measuring the intergranular stresses). The above applications to transport over a gravity bed over so great a range of density differences therefore constitute a severe test of the general correctness of the various inferences.

The original experiments unfortunately have not as yet been repeated by others using improved apparatus. So the curves of figures 4 and 5 may need some modification in detail. In default of any other information, however, the values taken for the friction coefficient of bedload transport in the following discussion are those given by figure 4.

THE SUSPENDED TRANSPORT EFFICIENCY e_s OF SHEAR TURBULENCE

Mass-transfer theories on the suspension of solids by fluid turbulence are based on the analogy of momentum transfer. Since no density differences are involved in the latter, the reasoning can justifiably be kinematic. To extend the same reasoning to solids having an appreciable excess weight it is necessary to define the solids by their kinematic property of fall velocity.

This is in effect to treat the solids as little fishes of zero excess weight swimming perpetually downward relative to the fluid at the given fall velocity. With the aid of certain assumptions about the turbulence, this kinematic approach succeeds in predicting the decrease in concentration of the fishes with increase of distance from the boundary.

This approach fails however, inevitably, to predict any limit to the total weight of fishes which a given turbulent flow can carry in suspension. For it ignores the reality that to maintain a suspension of heavier solids the turbulence must exert an upward stress equal to the excess weight of all the solids present over unit bed area. Clearly, no such upward stress is necessary to support the fishes.

That a limit to the suspended load must exist is indisputable. Otherwise rivers as we know them could not exist, for no deposition of suspended material could occur and no suspendable bed material could remain unsuspended. From the dynamic viewpoint it is evident that the suspension of heavier solids requires some limited proportion of the internal energy of the turbulence to be organized in such a way that it is capable of doing work in supporting the excess weight of the suspension. This means that e_s must have a certain limiting value.

In an attempt to predict this limit, conventional theory assumes that the necessary datum concentration close to the gravity boundary is given by that of the solids transported along the boundary as bedload, that is, by another mechanism. This assumption implies that a maintained suspension requires the presence of a bedload and cannot continue without it. If so, the hydraulic transport of solids in suspension through closed ducts would become inexplicable. For here the development of a bedload is deliberately prevented by working within a limit of concentration beyond which a bedload begins to develop.

A further weakness of the above assumption is that it makes serious difficulties when the suspended material is small in size. Such material has to be arbitrarily excluded from consideration, as "washload."

The following alternative dynamic concept avoids these difficulties and at the same time predicts a quantitative limit to e_s of approximately the required value.

Isotropic turbulence cannot by definition be capable of exerting any upward directed stress which could support a suspended load against gravity. For any suspended solid must experience over a period of time a downward flux of eddy momentum equal on the average to the upward flux. A swarm of solids would be dispersed equally in all directions by diffusion along uniform concentration gradients, but the center of grav-

ity of the swarm would continue to fall toward a distant gravity boundary.

The center of gravity of a swarm of solids suspended by shear turbulence, on the other hand, does not fall toward the gravity shear boundary. The excess weight of the solids remains in vertical equilibrium. It follows therefore that the anisotropy of shear turbulence must involve as a second-order effect a small internal dynamic stress directed perpendicularly away from the shear boundary. In other words, the flux of turbulent fluid momentum away from the boundary must exceed that toward it.

One might infer intuitively, on the analogy of solid physics, that the magnitude of this stress would be of the same order as that of the shear stress causing it. Although a stress of this order would account for the observed phenomenon of suspension, it would be too small to have been distinguished instrumentally from the far greater superimposed fluid pressures, static and dynamic.

Instruments used to measure the three components $\bar{u}'$, $\bar{v}'$, and $\bar{w}'$ of the internal velocity fluctuations are incapable of distinguishing to from fro. They give only the overall root-mean-square values. And for mathematical simplicity it has been assumed that the fluctuations in shear turbulence are as symmetrical in the to-and-fro sense as they must be in isotropic turbulence. That is, the root-mean-square values of the separate positive and negative parts of a complete velocity fluctuation have been assumed symmetrical.

This symmetry seems unlikely to be true of motion in boundary shear turbulence in the direction normal to the boundary. Photographs such as that in figure 3.6 of Prandtl (1952), though admittedly of artificially induced turbulence, show the normal motion to be highly asymmetrical.

The basic features disclosed by this photograph are as sketched here in figure 6. The turbulence appears to be initiated and controlled by a process akin to the generation of surface waves by a strong wind. An upwelling on the part of a minor mass of less turbulent boundary fluid intrudes into an upper, faster moving layer, where its crest is progressively torn off, like spray, and mingles with the upper layer. Corresponding motion in the reverse sense are absent or inappreciable.

Since there cannot be a net normal transport of fluid, the return flow must be effected by a general sinking toward the boundary on the part of a major mass of surrounding fluid. Hence the velocity v'_{up} of the upwelling exceeds the downward velocity v'_{dn} of the return flow, as sketched in figure 7.

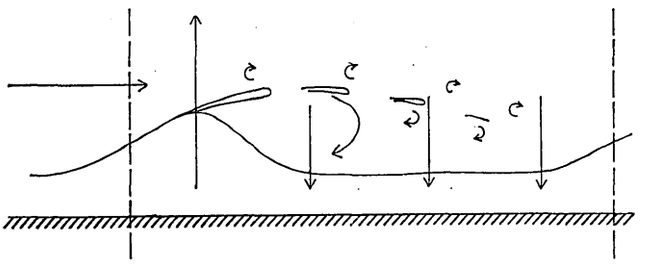

FIGURE 6.—Characteristic fluid motion close to the boundary, as inferred from photograph (Prandtl 1952, fig. 3.6) of the onset of boundary turbulence.

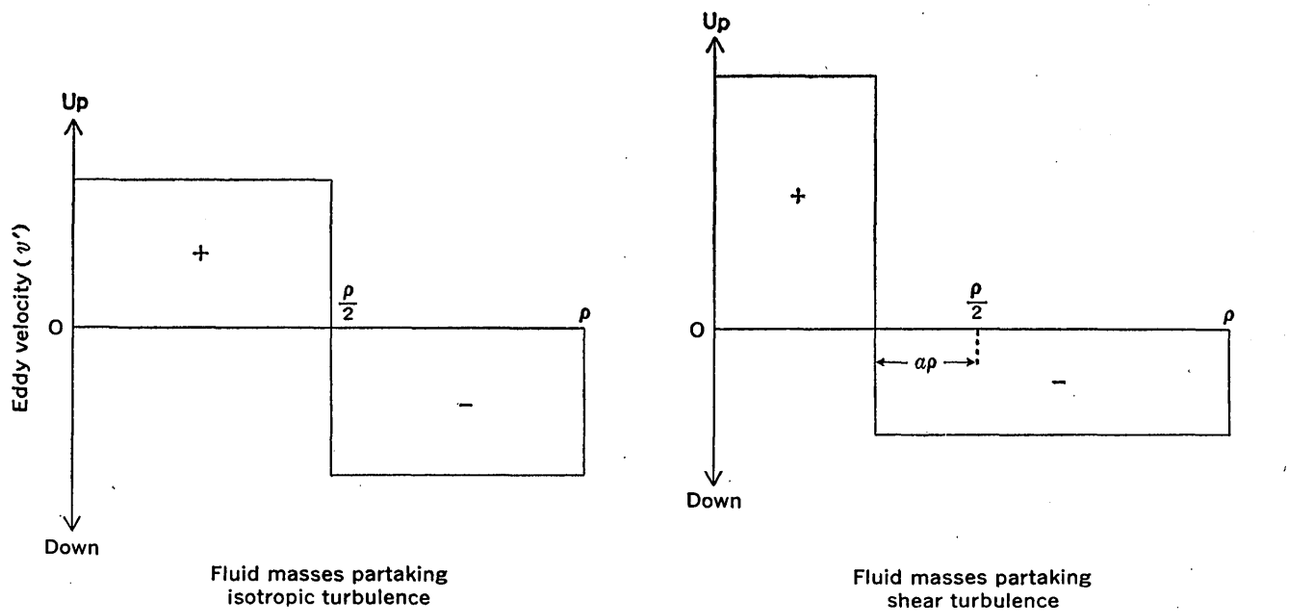

FIGURE 7.—Schematic diagram showing postulated asymmetry in the normal eddy velocity components of shear turbulence. In both isotropic and shear turbulence, continuity requires that the total discharge, as given by the positive and negative areas, must be zero. In isotropic turbulence the symmetry makes the upward and downward elements of momentum flux equal, but the asymmetry in shear turbulence gives a residual upward momentum flux.

Consider a representative unit volume of fluid within the boundary region where the normal fluctuations are decreasing toward the boundary. Inside this unit volume let a minor mass $\rho(\frac{1}{2}-a)$ be moving upward at root-mean-square velocity v'_{up}, and the remaining major mass $\rho(\frac{1}{2}+a)$ be moving downward at a velocity v'_{dn}, the asymmetry a being positive.

The total normal momentum must be zero, so

$$\frac{v'_{dn}}{v'_{up}}=\frac{1-2a}{1+2a}$$

but the normal momentum fluxes, per unit area of a shear plane, are unequal. There results a residual unidirectional momentum flux f, upward into the body of the flow, of magnitude

$$f=\rho v'^2_{up}\frac{1-2a}{2}-\rho v'^2_{dn}\frac{1+2a}{2}=\rho v'^2_{up}\cdot 2a\frac{1-2a}{1+2a} \qquad (14)$$

balanced below by an equivalent excess of mean static pressure at the boundary.

If the velocity v'_{up} is determined by the shear stress τ, then for a given τ the flux f has a limiting maximum value when the asymmetry $a=\frac{1}{2}(\sqrt{2}-1)=0.207$.

Shear turbulence results, broadly, from a general dynamic flow instability. And again broadly, within the region of its generation, the intensity of any dynamic instability disturbance proceeds spontaneously to the limit set by the approach of the energy losses involved to the energy supply. It is to be expected therefore that this particular energy loss, associated with f, would be maintained at its maximum value. So there is a reasonable probability that the asymmetry a has the critical value 0.207 within the boundary region. It must, however, decrease toward zero through the body of the flow as the turbulence approaches isotropy with increasing distance from the boundary.

The relation in equation 14 can be expressed in terms of the overall mean measured velocity $\bar{v}'$ by addition

$$\bar{v}'^2=v'^2_{up}\frac{1-2a}{2}+v'^2_{dn}\frac{1+2a}{2}=v'^2_{up}\frac{1-2a}{1+2a} \qquad (15)$$

whence

$$f=2a\rho\bar{v}'^2=0.414\rho\bar{v}'^2 \text{ on the above assumption}$$

The measured quantity $\bar{v}'$ has been found to increase from zero at the boundary to a sharp maximum, and then to decrease progressively with distance from the boundary (Laufer, 1954; Townsend, 1955). The ratio $\bar{v}'_{max}/u_*$ appears to be in the neighborhood of unity.

Thus the normal momentum flux entering the body of the flow above the plane of $\bar{v}'_{max}$ is

$$f=0.414\rho\bar{v}'^2_{max}\approx 0.414\tau$$

This value would be well below the limit of sensitivity of Laufer's manometer. So the excess reaction pressure at the boundary could not have been detected. Significantly however an energy loss toward the boundary by pressure transport was inferred from the energy balance drawn up. (See also Townsend, 1955, p. 217 and fig. 9.12.)

The propagation velocity of the flux f being $\sqrt{f/\rho}$, the supply of lifting power to the body of the flow is

$$f\sqrt{f/\rho}=(2a)^{3/2}\rho\bar{v}'^3=0.266\rho\bar{v}'^3_{max} \qquad (16)$$

It remains to express this relation in terms of the whole power supply $\omega=\tau\bar{u}$, from the rather inadequate experimental data.

According to Laufer's work the ratio $\bar{v}'_{max}/u_*$ varies with the Reynolds number of the flow, and is approximately 1.0 at $\mathbf{R}=3\times10^4$ and approximately 1.1 at $\mathbf{R}=3\times10^5$. This ratio being denoted by b and the flow coefficient $\bar{u}/u_*$ by c, the suspension efficiency e_s should be given by

$$e_s=\frac{f\sqrt{f/\rho}}{\tau\bar{u}}=0.266b^3/c \qquad (17)$$

At flow velocities u of the same order, b would increase with increasing flow depth. And since c increases likewise, it is possible that b^3/c may remain constant over a wide range of conditions.

Experimental flume conditions being taken as a standard, since they cover approximately the same experimental range of $\mathbf{R}$, b may be put at say 1.03, and c appears to range only between 16 and 20 for high-stage flows and for the sand range of grain sizes. Putting $c=18$,

$$e_s=\frac{0.266\times1.1}{18}=0.016 \qquad (17a)$$

Laufer's measurements refer to flows past smooth boundaries, and the effect of boundary roughness on the ratio b appears to be uncertain, as is also the effect of the presence of transported solids. However, for test purposes I decided to ignore these uncertainties and to assume that the suspension efficiency e_s has the universally constant value 0.015 for fully developed suspension by turbulent shear flow. This assumption gives the numerical coefficient in the second term of equation 9 the round figure of $\frac{2}{3}\times0.015=0.01$.

It may of course be fortuitous that this value makes the general transport relation in equation 9 accord surprisingly well with the comprehensive range of transport data to be presented later. From the river evidence the figure might be 25 percent larger but no more.

The postulated upward lifting power supplied to the flow body from below would also account for the

hitherto unexplained persistence of secondary circulations in long straight channels, by creating large-scale instabilities of the same nature as density instabilities due to thermal gradients.

Incidentally, the theory may shed some light on the truth of the legend that the surface of a stream is slightly raised in the center. If the stream cross section is dish shaped or trapezoidal, so that the local τ is negligible at the sides, and if the stream is unladen with suspended sediment, the maximum predicted excess height in midstream would be $f/\rho g \approx 0.4dS$. In natural rivers this maximum would rarely amount to 10^{-3} feet. It would be still less if the excess head were relieved by secondary circulations.

Since writing this section I have seen Prof. S. Irmay's highly relevant paper (Irmay, 1960). In the latter, my postulated normal stress f is predicted mathematically in terms of acceleration, by an entirely different approach along the lines of Reynolds' (1895) treatment of the Navier Stokes equations.

Irmay has shown that the Reynolds approach leads to a mean acceleration A, the normal component of which, in the present notation, is

$$A_y=\frac{d(\bar{v}'^2)}{dy} \quad \text{(Irmay's equation } 11_3\text{)}$$

Hence if Y is the flow depth from the boundary up to the no-shear plane, the upward momentum flux f is given by

$$f=\rho\int_0^Y A_y dy=\rho\bar{v}'^2, \text{ since } v'=0 \text{ at the boundary}$$

This flux is shown to be generated in the region of maximum $\bar{v}'$ close to the boundary (see Irmay's fig.4). My own approach appears to explain the mechanism of its generation there.

As can be seen from Irmay's figure 2, based on Laufer's data for $\mathbf{R}=3\times10^4$,

$$f=\rho\bar{v}_y'^2=\text{approx. } 0.375\tau$$

which compares well with my value of approximately 0.41τ.

Thus my conclusions receive strong independent support. In the light of these new ideas it would seem that the basis of the conventional theory of suspension may need serious reassessment. For the existence, inherent in shear turbulence, of an upward fluid stress appears incompatible with theories purporting to explain suspension in the absence of such a stress.

Two immediate implications of Irmay's more detailed analysis may be noted here.

1. The normal concentration profile of suspended solids is related to the rate of decrease with distance from the boundary of the normal momentum flux $f_y=\rho\bar{v}_y'^2$ as modified by the transfer of upward momentum to the solids.

   If C_y is the weight of suspended solids per unit volume at distance y from the boundary, the work rate needed to maintain the suspension of the solids in a layer dy is C_yVdy. The fluid lifting power is $-d(f^{3/2})\sqrt{\rho}$. Whence

$$C_y=-\frac{1}{\sqrt{\rho}V}\frac{d(f^{3/2})}{dy}=-\frac{\rho}{V}\frac{d(\bar{v}_y'^3)}{dy}$$

   The required modification of the $\bar{v}'$ profile may be deducible from the measurable modification of the Karman constant by a suspension of solids.

2. The no-shear region in Laufer's experiments was that of the central axis of a closed duct. So the normal fluctuations remained finite there. At the free surface of an open flow the normal fluctuations are inhibited. The dynamic Reynolds stress $\rho\bar{v}'^2$ must therefore fall sharply to zero as it does at the shear boundary below, being converted into an excess of static head. Thus the whole integral

$$f=\rho\int_0^Y Aydy$$

   needs to be taken to an upper limit just below the free surface.

   In the thin intervening zone there must exist a large negative acceleration, downward away from the surface, possibly of the same order as the large positive acceleration, found to exceed $2g$, at the shear boundary.

   This seems likely to account for the hitherto unexplained phenomenon observable in flume experiments on sediment transport, namely the inability of transported solids ever to touch the actual surface film, together with the existence of a thin layer of relatively sediment-free fluid immediately beneath the surface.

CRITICAL FLOW STAGES FOR SUSPENSION

It is reasonable to suppose that no solid can remain suspended unless at least some of the turbulent eddies have upward velocity components v'_{up} exceeding the fall velocity V of the solid. The turbulence has a spectrum of such velocity components, of which v'_{up} is the mean. Some eddies have greater upward velocities and some less. Hence the stages marking the threshold and full development of suspension should be definable by critical values of the ratio v'_{up}/V, the threshold occurring at some value less than unity and full development at some higher value.

From equation 15, $v'_{up}=1.56\bar{v}'$ when $a=0.207$. And $\bar{v}'$ varies as the shear velocity $\sqrt{\tau/\rho}$. The Laufer (1954)

data being used as before, $\overline{v}'$ appears to have an average value of about $0.8u_*$ over the flow depth. Whence as a tentative approximation we can write $\overline{v}'=1.25\sqrt{\tau/\rho}$. So unit value of the ratio v'_{up}/V can be defined by $1.25^2\tau=\rho V^2$. Substituting $\tau=\theta_s(\sigma-\rho)gD$,

$$\theta_s=0.64\frac{V^2}{gD}\frac{\rho}{\sigma-\rho}$$

$$=0.4\frac{V^2}{gD}\text{ for quartz-density grain in water} \quad (18a)$$

Since the fall velocity V becomes proportional to $\sqrt{D}$ for all large grains exceeding about 2 mm, θ_s should remain constant for all large material irrespective of size. V being 20 centimeters per second for $D=2$ mm, $\theta_s\approx 0.8$ for all such material.

On the other hand, V^2/gD decreases rapidly with decrease of grain size, as is shown in figure 8.

Here the θ values for the threshold of bed movement, according to Shields (1936), are also shown. It can be seen that suspension is likely to be appreciable at the threshold of bed movement when the grain size is 0.25 mm or less, and to become fully developed at that early stage when the grain size is 0.1 mm or less. By contrast, grains larger than 1 mm are unlikely to be suspended at all until the bed stress is many times greater.

The above applies to grains of uniform size. The suspension of natural materials of heterogeneous size involves the spectra of both eddy velocity and fall velocity. Over the transition range of stages, suspension must begin at an earlier stage than that for uniform material of the same mean size, the smaller materials being suspended first.

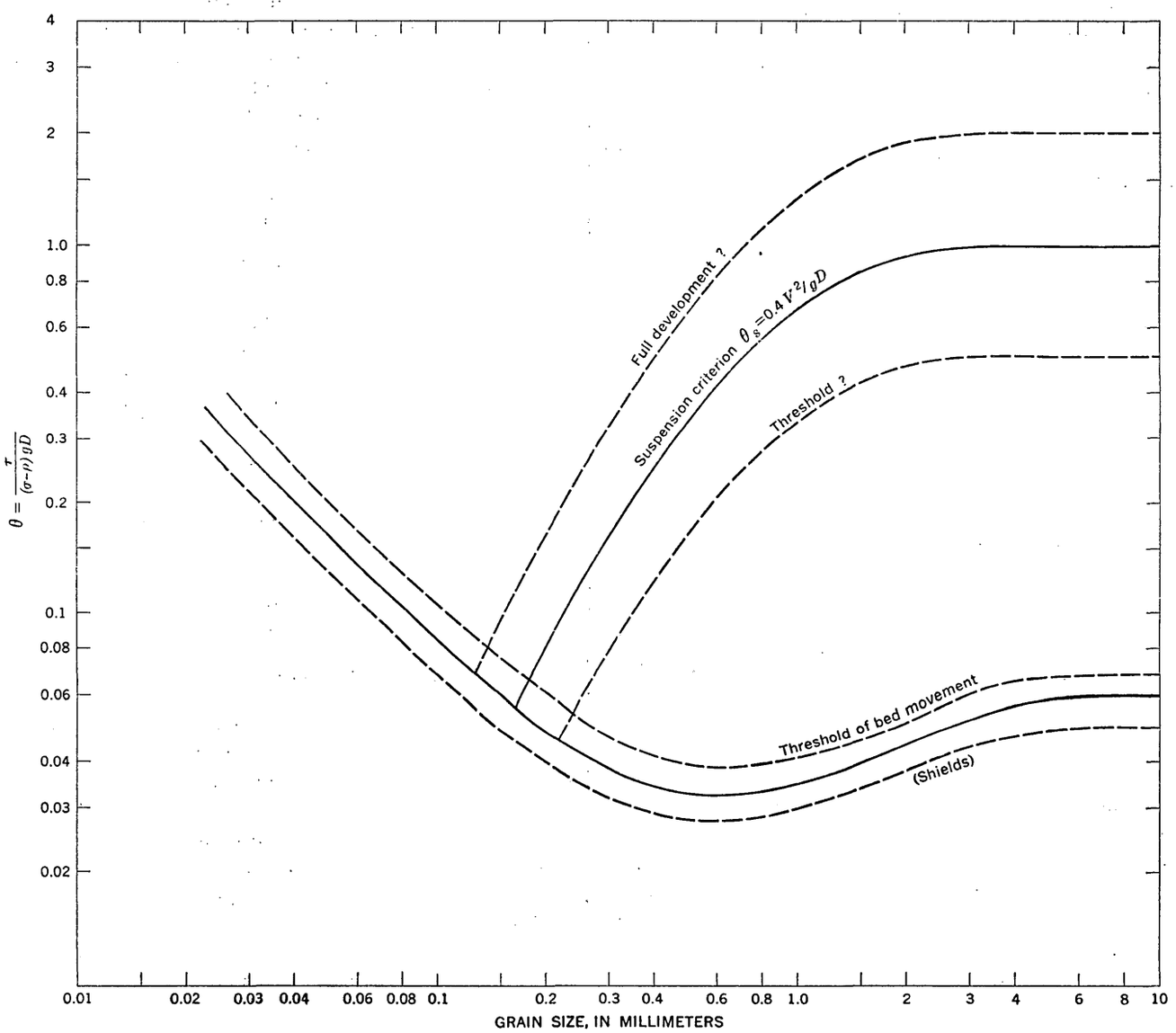

FIGURE 8.—Theoretical values of the suspension criterion $\theta_s=V^2/gD$ together with Shields' (1936) values of θ at the threshold of bed movement.

An interesting and informative test of the generality of equation 18*a* is afforded by applying it to the atmospheric transport of solids. From the derivation given, equation 18*a* can be written as

$$V^2=1.5\tau/\rho$$

where ρ is now 1.2×10^{-3} grams per cubic centimeter.

If τ is taken as 10 dynes per square centimeter for a reasonably strong ground wind over an open sand surface, then $V=1.14$ meters per second. And this is the fall velocity in air of 0.14-mm quartz grains. Hence suspension should not be appreciable in such a wind, for grains larger than say 0.2 to 0.25 mm in size.

We should expect, therefore, that the wind would carry away grains smaller than this, scatter them over wide areas, and leave behind local dune accumulations having a dominant size never less than 0.2 mm (except in specially sheltered spots).

This is precisely what is found. The finest dune sand found on open country has a dominant size seldom less than 0.2 mm—usually 0.25 mm.

THE EFFECTIVE FALL VELOCITY V FOR SUSPENSION OF HETEROGENEOUS SEDIMENTS

The fall velocity V enters as a factor of the work rate $m_s'gV$ (equation 4) required to maintain the suspension of an excess weight $m_s'g$ of solids. It follows that if the suspended solids are heterogeneous in size, the work rate is given by the arithmetic mean of the fall velocities

$$V=\frac{\sum(pV_p)}{\sum p} \qquad (19)$$

where p is the weight of any individual constituent grade whose fall velocity is V_p.

The effective mean fall velocity V of a heterogeneous suspension (equal to $\Sigma(pV_p)$ when Σp is made unity and p becomes a numerical proportion) may be so much larger than the fall velocity of a solid of size $D_{50\text{ percent}}$ on the conventional cumulative diagram that it cannot always be assumed equal to it even as a first approximation. It must be remembered that the cumulative diagram is merely an arbitrary device for representing the size distribution and takes no account of any physical effect of grain size as such. It is simply Σp plotted against D_p.

$V=\Sigma(pV_p)$ is comparable to the arithmetic mean grain size

$$D_a=\sum(pD_p)$$

But since V_p is a varying function of D_p, V can only be equal to V_{Da} over the narrow range of sizes within which V_p is approximately proportional to D_p—that is, around $D_a=0.6$ mm for quartz-density grains in water.

Some idea of the magnitude of the discrepancy between $V=\Sigma pV_p$ and $V_{D50\text{ percent}}$ can be got from the following examples, taken from U.S. Geological Survey analyses of suspended river sediments.

Rio Grande at Otowi Bridge, N. Mex.[1] *(5–12–48)*

Size limit (mm)	Percent finer	p	D_p (mm)	pD_p (mm)	V_p (cm per sec)	pV_p (cm per sec)
4	100					
		0.012	3.0	0.036	24.0	0.29
2	98.8					
		.048	1.5	.072	22.0	1.06
1	94.0					
		.07	.71	.050	10.0	.70
.5	87					
		.09	.35	.032	5.0	.45
.25	78					
		.20	.176	.035	1.9	.38
.025	58					
		.16	.088	.014	.6	.096
.0625	42					
		.22	.0312	.0069	.08	.0176
.0156	20					
		.07	.0078	.00054	.005	.00035
.0039	13					
		[2].12				
Total		1.00		D_a=0.245 mm		V=3.0 cm per sec

[1] $D_{50\text{ percent}}$=0.088 mm, and $V_{D\ 50\text{ percent}}$ would be 0.6 cm per sec. Whereas, V=3 cm per sec is five times bigger. $D_V=D_a$=0.245 mm, corresponding to approximately $D_{50\text{ percent}}$. The three biggest grades together constitute only 6 percent of the suspended material, but contribute 66 percent to the value of V.
[2] Fines neglected.

Elkhorn River at Waterloo, Nebr.[1] *(3–26–52)*

Size limit (mm)	Percent finer	p	D_p (mm)	pD_p (mm)	V_p (cm per sec)	pV_p (cm per sec)
0.5	100					
		0.04	0.35	0.014	5	0.2
.25	96					
		.19	.176	.0335	1.9	.36
.125	77					
		.15	.088	.0132	.6	.09
.0625	62					
		.13	.044	.0057	.16	.0208
.0312	49					
		.21	.022	.0046	.04	.0084
.0156	28					
		.04	.011	.00044	.01	.0004
.0078	24					
		.06	.0055	.00033	.0025	.00015
.0039	18					
		[2].18				
Total		1.00		D_a=0.0718 mm		V=0.68 cm per sec

[1] $D_{50\text{ percent}}$=0.033 mm, and $V_{D\ 50\text{ percent}}$ would be 0.09 cm per sec. V is 7.6 times bigger. D_V=0.092 mm, which is 1.3 times D_a. D_V corresponds to approximately $D_{70\text{ percent}}$.
[2] Fines neglected.

Rio Puerco near Bernardo, N. Mex.[1] *(8–10–59)*

Size limit (mm)	Percent finer	p	D_p (mm)	pD_p (mm)	V_p (cm per sec)	pV_p (cm per sec)
1.0	100					
		0.002	0.71	0.00142	10	0.02
.5	99.8					
		.006	.35	.00210	5	.03
.25	99.2					
		.041	.176	.00720	1.9	.078
.125	95.1					
		.083	.088	.00555	.6	.049
.0625	86.8					
		.153	.044	.00670	.16	.0244
.0312	71.5					
		.101	.022	.00220	.04	.0040
.0156	61.4					
		-------	.011	.0011	.01	.001
.0078	51.4					
		.014	.0055	.00007	.0025	.000035
.0039	50.0					
		[2].50				
Total		1.00		D_a=0.026 mm		V=0.206 cm per sec

[1] $D_{50\text{ percent}}$=0.0039 mm, and $V_{D50\text{ percent}}$ would be 0.0013 cm per sec. V is 160 times bigger. D_V=0.016 mm, which is smaller than D_a. D_V corresponds to approximately $D_{75\text{ percent}}$. The four biggest grades together constitute only 5 percent of the suspended material, but contribute 60 percent to the value of V.
[2] Fines neglected.

The comparatively large discrepancies between V and $V_{D50\text{ percent}}$ in the above examples refer to wide size distributions, and to those which extend well into the Stokes law range of sizes. Naturally, the discrepancy diminishes with decrease of distribution width (see following example).

Rio Grande at Cochiti, N. Mex.[1] *(6–17–58)*

Size limit (mm)	Percent finer	p	D_p (mm)	pD (mm)	V_p (cm per sec)	pV_p (cm per sec)
2.0	100	.01	1.5	.015	22	22
1.0	99	.249	.71	.177	10	2.49
.5	74.1	.455	.35	.158	5	2.27
.25	28.6	.238	.176	.042	1.9	.35
.125	4.8	.012	.088	.0011	.6	.01
.0625	-------	[2].036				
Total	-------	1.00	-------	D_a=0.363 mm	----------	V=5.34 cm per sec

[1] $D_{50\text{ percent}}$=0.34 mm, and $V_{D50\text{ percent}}$ would be 4.7 cm per sec. So V is only 1.3 times larger. D_V=0.37 mm corresponds to approximately $D_{50\text{ percent}}$.
[2] Fines neglected.

The effective mean fall velocity V thus depends both on the distribution of p versus D and on the position of this relative to the curve of fall velocity versus D. It therefore bears no general relationship to $V_{D50\text{ percent}}$.

It should perhaps be emphasized here that the effective mean fall velocity $V=\sum pV_p$ is involved in the transport of suspended load only. It is not involved in the transport of bedload. Moreover, the summation of pV_p refers to the actual size distribution of the suspended material. V may be considerably smaller than the value computed from the overall size distribution of the whole material.

THE EFFECTIVE MEAN GRAIN SIZE D FOR HETEROGENEOUS BEDLOADS

The bedload friction coefficient $\tan\alpha$ and the dimensionless bed-stress parameter $\theta=\tau/(\sigma-\rho)gD$ are both functions of D. The questions therefore arise, What kind of mean value of D should be taken as representative of the bedload, and on what size distribution should this mean be computed?

Since the physical effects of the magnitude of D are relevant, the arithmetic mean $\sum pD_p$ seems more likely to be representative than the arbitrary $D_{50\text{ percent}}$ which takes no account of the effects of magnitude. Ideally, the size distribution should be that of a sample of the bedload itself; but no such sample can be isolated experimentally. It seems reasonable to assume the closest practicable approximation to be for a river a sample of the bed surface material, and for a laboratory flume a sample of the whole experimental material.

WASHLOAD

An examination of the final columns of the above tabular examples shows that in the first three examples the contribution to the total suspension work rate made by the whole finer 50 percent of the suspended load is respectively 3.8, 1.3, and (by estimation) less than 0.4 percent.

These values appear to give the so-called washload a rational physical meaning. It is merely that part of the suspended load whose contribution to the total suspension work rate is relatively negligible. If relative negligibility is placed at 1 percent, the distinguishing grain sizes in the above three examples would be respectively 0.08 mm, 0.02 mm, and 0.07 mm approximately.

Further, the empirical definition of washload as fine suspended material which is not present on a riverbed in appreciable quantity is also consistent with the foregoing ideas. As can be seen from figure 8 material of this order of size is so readily maintained in suspension that it would be unlikely to become deposited even at low river stage anywhere other than in stagnant backwater.

It might at first sight be concluded that since the finer grades of a suspended load make negligible contribution to the suspension work rate, the transport rate of the suspended load must be indeterminate But this conclusion would be wrong. Suppose we were to double the transport concentration C—and thereby the transport rate—by adding very fine material, which has so small a fall velocity that it contributes nothing to the suspension work rate. The effect of this addition would be to halve all the frequencies p of the larger contributing grades. Hence $\sum pV_p$ is halved. So, by equation 8 the predicted transport rate would be doubled, as required by the original supposition.

THE FINAL TRANSPORT RATE RELATIONSHIP

We can now amplify the outline relationship in equation 9 to give it a sufficiently practical form to permit a trial comparison with the measured data from both flume experiments and natural rivers.

Adequate flow depth and fully turbulent flow being assumed, equation 9 reduces to

$$i=\omega\left(\frac{e_b}{\tan\alpha}+0.01\,\frac{\bar{u}}{V}\right) \qquad (20)$$

where $i=\frac{\sigma-\rho}{\sigma}j$=0.62 times the conventional transport rate by dry weight for quartz-density grains in water; ω=stream power $\rho dS\bar{u}$ in units consistent with i; e_b is given in figure 3; $\tan\alpha$ is given in figure 4; V=effective fall velocity ΣpV_p for the suspended material; and

the coefficient 0.01 against the second suspension term is the theoretical suspension efficiency 0.015 reduced by the factor 2/3 on account of the stream power already dissipated in bedload transport.

For mean bed grain sizes D_a less than 0.5 mm, $e_b/\tan\alpha$ can as a first approximation be taken as 0.17 for θ less than unity.

Equation 20 can of course be written as

$$I=\Omega\left(\frac{e_b}{\tan\alpha}+0.01\,\frac{\bar{u}}{V}\right) \tag{20a}$$

in terms of the whole width of the flow.

If $C'=0.62C$ is used for the transport concentration by immersed weight, equation 20 may be put in the alternative form

$$C'=S\left(\frac{e_b}{\tan\alpha}+0.01\,\frac{\bar{u}}{V}\right) \tag{20b}$$

or

$$\frac{i}{\omega}=\frac{C'}{S}=\left(\frac{e_b}{\tan\alpha}+0.01\,\frac{\bar{u}}{V}\right)$$

The ratio

$$i_s/i_b=\frac{\text{suspended transport rate}}{\text{bedload transport rate}}=0.01\,\frac{\bar{u}\tan\alpha}{Ve_b} \tag{21}$$

This equation is approximately equal to $0.06\,\frac{\bar{u}}{V}$ for grains smaller than 0.5 mm.

This ratio should increase with decreasing grain size. For a given overall size distribution it should also increase with increasing stage, but this increase may be masked by a progressive increase in V as larger grains are brought into suspension.

Inadequate flow depth, however, should cause the bedload rate i_b to increase disproportionately with increasing stage, by a factor of 3 or less.

The load ratio $\frac{\text{suspended load}}{\text{bedload}}$, that is, the ratio of the quantities of suspended and unsuspended solids present over unit bed area, appears to be considerably smaller. The suspended load is $i_s/\bar{u}$ and the bedload is i_b/U_b, where $U_b/\bar{u}=e_b$, which is of the order of 0.13 (fig. 3). The load ratio is therefore

$$e_b\frac{i_s}{i_b} \tag{22}$$

Clearly, if the bedload travels slower than the suspended load the quantity of bedload present must be correspondingly greater. This emphasizes the need to distinguish between transport concentrations and spatial concentrations. The present looseness of definition tends to a confusion of thought.

Equations 20, 20a, and 20b can be written in the alternative dimensionless forms

$$\frac{i}{\omega}\frac{V}{\bar{u}}=\frac{I}{\Omega}\frac{V}{\bar{u}}=\frac{C'}{S}\frac{V}{\bar{u}}=\frac{e_bV}{\tan\alpha\bar{u}}+0.01 \tag{20c}$$

The equivalent terms on the left are now the proportion of stream power expended in sediment transport if the whole of the load were suspended. This approximates to reality when the bedload term on the right is small compared with 0.01, that is, when $V/\bar{u}$ is small.

If we neglect the bedload work, the proportion $\frac{i}{\omega}\frac{V}{\bar{u}}$ of stream power expended in sediment transport is constant, as was suggested by Rubey (1933, p. 503). Rubey's values for this proportion, inferred empirically from river data, were rather larger, around 0.025 instead of 0.01. This is understandable because the bedload work element was not taken into consideration and because the effective fall velocity V was estimated in a different way.

EXISTING FLUME DATA

LIMITATIONS AND UNCERTAINTIES

Very few of the many laboratory transport-rate measurements extend to the higher stages with which we are here concerned and which seem to be prevalent in many rivers. Although now half a century old, Gilbert's (1914) work still provides the majority of the available data.

This data deficiency may be attributed in part to a lack of appreciation of the real conditions the experiments were aimed at reproducing; but it seems to be due mainly to two outstanding experimental weaknesses: (*a*) underestimation of the pumping capacities required, and consequent inability to maintain adequate flow depths at the higher stages; and (*b*), resulting from *a*, increasingly serious disturbances of the flow associated with unnaturally high Froude numbers at inadequate flow depths.

Several uncertainties arise in the interpretation of the few relevant sets of data available:

1. A large scatter exists within most sets of data. No serious investigation has been made into the cause. So it has remained uncertain how far this scatter may be systematic. A correlation with variations of flow depth has long been known qualitatively to exist, but unfortunately—
2. We have no reliable way of estimating the proper reduction factor to be applied in the evaluation of the tractive stress τ and of the available power ω to make allowance for ineffective wall drag in rectangular flumes.

3. Although in some sets of data the $D_{50\,\text{percent}}$ grain size of the total transported solids is given, together with that of the whole stock of experimental material, the size distributions of the transported solids are omitted in all sets of data. Further, even were the transported distributions to be given, it would be impossible in such shallow flow depths to make any reliable estimate of the size distributions of the suspended loads as distinct from the bedloads. Hence the effective fall velocity V of the suspended loads cannot be determined with any accuracy.

   In this respect the data obtained from natural rivers is likely to be more relevant. For over the greater prevailing flow depths the material collected by a sampler and its size distribution have reasonable likelihood of representing the suspended load alone.

   Similarly, no information is available as to the mean size of the bed-surface grains as an indication of the mean bedload size in flume experiments. Hence any estimate of the effective value of the bedload criterion $\theta=\frac{\tau}{(\sigma-\rho)gD}$ is open to some doubt. Since the data show that in general the mean transported size is smaller than that of the bed stock, it follows that the bed-surface size must be correspondingly larger. That is, the effective value of θ is likely to be smaller than that given by equating D to the measured mean stock size.

WALL DRAG AND FLOW DEPTH

I spent much time working through Gilbert's and other data in an attempt to discover what deduction factor applied to the tractive stress τ and the power ω, to allow for wall drag, would minimize the scatter in the plots of transport rate against ω. The factor which minimized the overall scatter throughout the range of stages was found to be $\frac{\text{bed width}}{\text{bed width}+1.6\ \text{depth}}$. This factor made a very marked improvement in the general alinement of the plotted points.

However, two significant facts emerged:

1. This reduction factor minimized the scatter in Gilbert's data not only over the range of sand sizes but also for the 5-mm pea gravel. Such a large allowance for wall drag for so rough a bed relative to the smooth flume walls appears to be unacceptable. Similarly for the finer grades, so large an allowance is also unacceptable over the lower, transitional stages in view of the much larger form drag exerted by the bed features.

2. In spite of this large adjustment of the omega values, the plotted points for the smallest depths (less than 0.1 ft) remained persistently discrepant. The nature of the discrepancy is clear from figure 9*B*, to which the points corresponding to these flow depths have been added as an example. It can be seen that the discrepancy would have increased with increasing stage had the smallest flow depths been maintained.

   The explanation is immediately apparent from what has been said under the heading "Effect of inadequate flow depth on the values of e_b." Just such a discrepancy is predicted by the theory; and indeed the theoretical prediction of the bedload efficiency e_b would have been invalidated by its absence.

This explanation removes any need to make an objectionably large allowance for wall drag. It now becomes reasonable to assume the relative wall drag to be considerably smaller for most experimental width to depth ratios.

On the other hand, the impression gained from the analysis of Gilbert's data, which includes some very small width to depth ratios, is that relative wall drag begins to increase rapidly when the width to depth ratio is made smaller than, say, 3.

These considerations have led me (*a*) to discard all Gilbert's data relating to the smaller flow depths on grounds of inadequate depth and to discard also all his data concerning width to depth ratios less than approximately 3; and (*b*) to plot the remaining measured transport rates against the power ω without making any allowance for wall drag. From the other, more recent experiments, the data, which all lie within these limits, have been plotted in their entirety.

Adequate flow depth being assumed measurable in terms of grain diameters, it would seem likely that Gilbert's entire data relating to the 5-mm pea gravel should be discarded on the ground of inadequate flow depth (around 14 diam only). I have however included these results for the sake of comparison.

Appreciable errors may well be introduced both by ignoring the effect of wall drag altogether and by assuming flow depths of 0.2 feet to be sufficiently large in relation to the effective thickness of the bedload zone, over the sand range of grain sizes, to validate the theory.

It seems to me strange that although research in rectangular flumes has been done for the past 50 years, no serious steps have been taken to clear up these uncertainties.

ESTIMATION OF APPROPRIATE FALL VELOCITY V

As previously pointed out, the experimental data show that in general the $D_{50\ \text{percent}}$ size of the total transported material, bedload plus suspended load, is considerably smaller than that of the whole bed stock. Hence the effective fall velocity V of the suspended load should also be smaller than that computed from the bed-stock data.

As a systematic approximation I have therefore assumed arbitrarily, in the absence of any factual information, that V has one-half the value given by ΣpV_p for the size distribution of the bed stock.

COMPARISON OF THE THEORY WITH THE EXPERIMENTAL FLUME DATA

In the following figures 9 to 13, the measured transport rates i are plotted against the power $\omega=\rho dS\bar{u}$. The plots are arranged in descending order of grain size.

Both the quantities i and ω have the dimensions of energy rates per unit of boundary area. The units used for both are pounds-feet per second-foot^2, equivalent to pounds per second-foot.

Superimposed are comparative plots of the theoretical values of i predicted according to equation 20. This equation, it should be remembered, was derived without recourse to information obtained from any flume experiment.

In plotting the factual data I have attempted to distinguish between reportedly "flat" or "smooth" beds and "dune" or "sand-wave" beds, and between these and "antidunes" occurring at the unnaturally high Froude numbers obtained in small-scale experiments. The difficulty here is that one condition merges gradually into the next, which makes the reported distinctions a matter of personal judgment. Reported "transition" conditions have been referred to the next lower condition. Thus "transition" from dune to flat is plotted as dune, and that from flat to antidune as flat.

The antidune condition would not have intervened had the experimental flow depths been larger, and it may be assumed, I think, that the beds would have remained flat. I have distinguished the antidune condition merely as an indication that the violent disturbances of the flow are likely to have rendered the measurements less reliable.

To complete the information, the corresponding values of $\bar{u}$ and θ are plotted in the following illustrations. In the absence of any information as to the actual mean sizes of the grains in transit close to the bed surface, the bedload grain size D in the denominator of θ has been given the value corresponding to the overall mean size of the material stock. The actual size D in θ may well be larger by a factor approaching 2.

GILBERT (1914) 5.0-mm PEA GRAVEL

Figure 9*A*

In terms of θ the highest stage reached is only 0.21, whereas according to figure 4 the critical stage should not have been reached until $\theta=0.26$. Hence this whole plot would seem to lie within the lower, transitional stages.

According to figure 8 it seems very likely that suspension would be negligible, the entire transport taking place as bedload. In consequence, the predicted values of i have been calculated using the first term only of equation 20.

The flow depth being around 14 grain diameters only, it would certainly have been inadequate at the higher stages. One would therefore expect the measured transport rates to have been too large by a progressively increasing factor, consistent with the plot.

GILBERT (1914) 0.787-mm SAND

Figure 9*B*

Depth range 75 to 110 diameters Approaches adequacy? Max $\theta=0.8$. Suspension possibly approaching ing full development (fig. 8). $V=0.18$ ft per sec. Average flow velocity $\bar{u}=3.5$ ft per sec over the higher stages. Ratio of suspended to bedload transport rates (i_s/i_b) approx 0.86 according to equation 21. That is, bedload transport rate still exceeds that of suspension. Load ratio $\frac{\text{suspended load}}{\text{bedload}}=e_b\frac{i_s}{i_b}=0.15$.

Critical stage: predicted from figure 4, $\theta=0.4$. From plot, θ between 0.3 and 0.5, as indicated by onset of flat beds, and between 0.4 and 0.5, as indicated by change of trend in data plot.

GILBERT (1914) 0.507-mm SAND

Figure 10*A*

Depth range 120 to 200 diameters. Probably adequate. Max $\theta=1.2$. Suspension probably fully developed (fig. 8). ($V=0.13$ ft per sec. Ratio $i_s/i_b=$approx 1.6 over the higher stages. Suspension beginning to dominate. Load ratio 0.29.

Critical stage: predicted from figure 4, $\theta=0.5$. From plot, flat beds, θ between 0.4 and 0.7; change of trend, θ between 0.5 and 0.6.

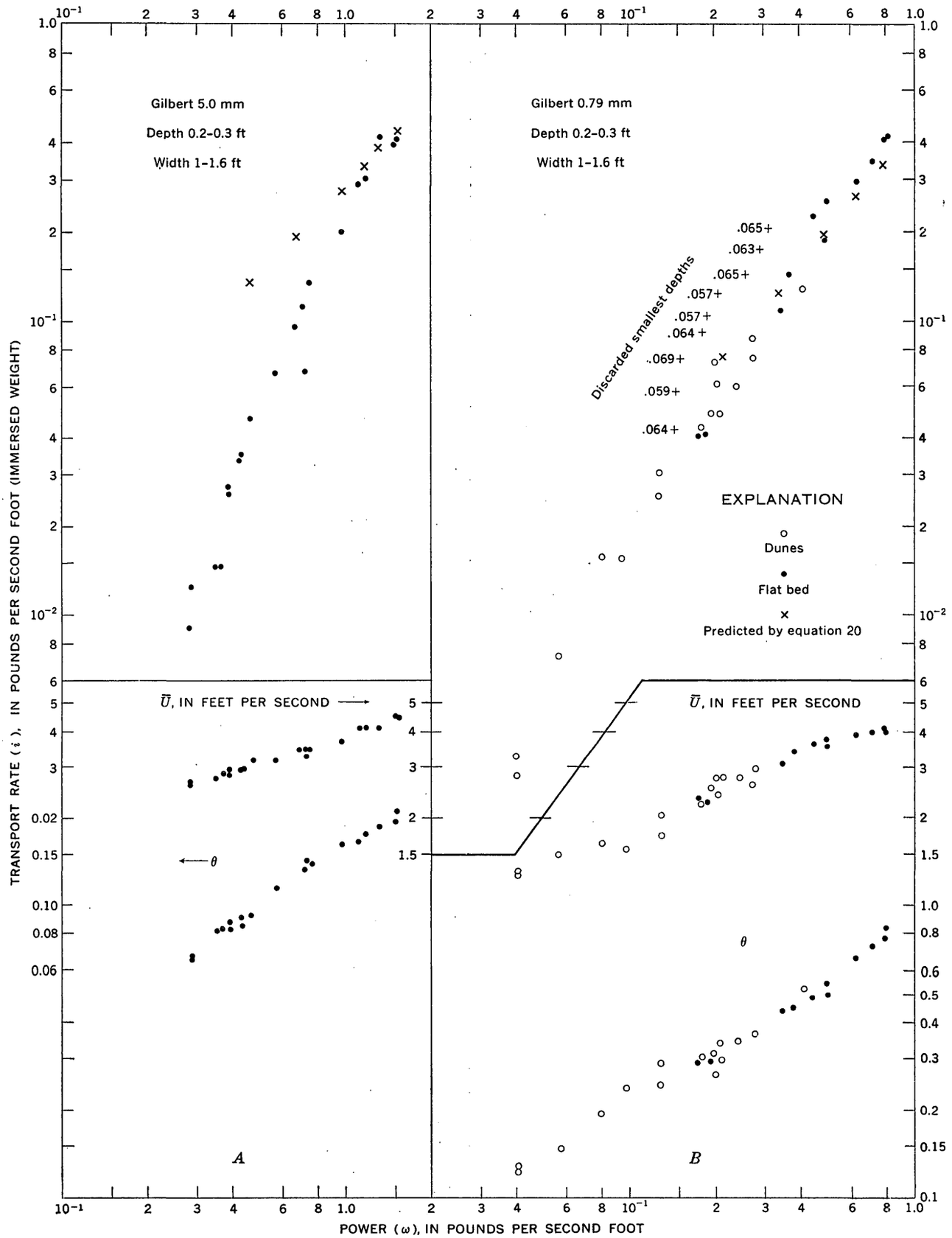

FIGURE 9.—Comparative plots of theoretical and experimental transport rates (flume experiments). *A*, Gilbert 5.0-mm gravel. *B*, Gilbert 0.787-mm sand.

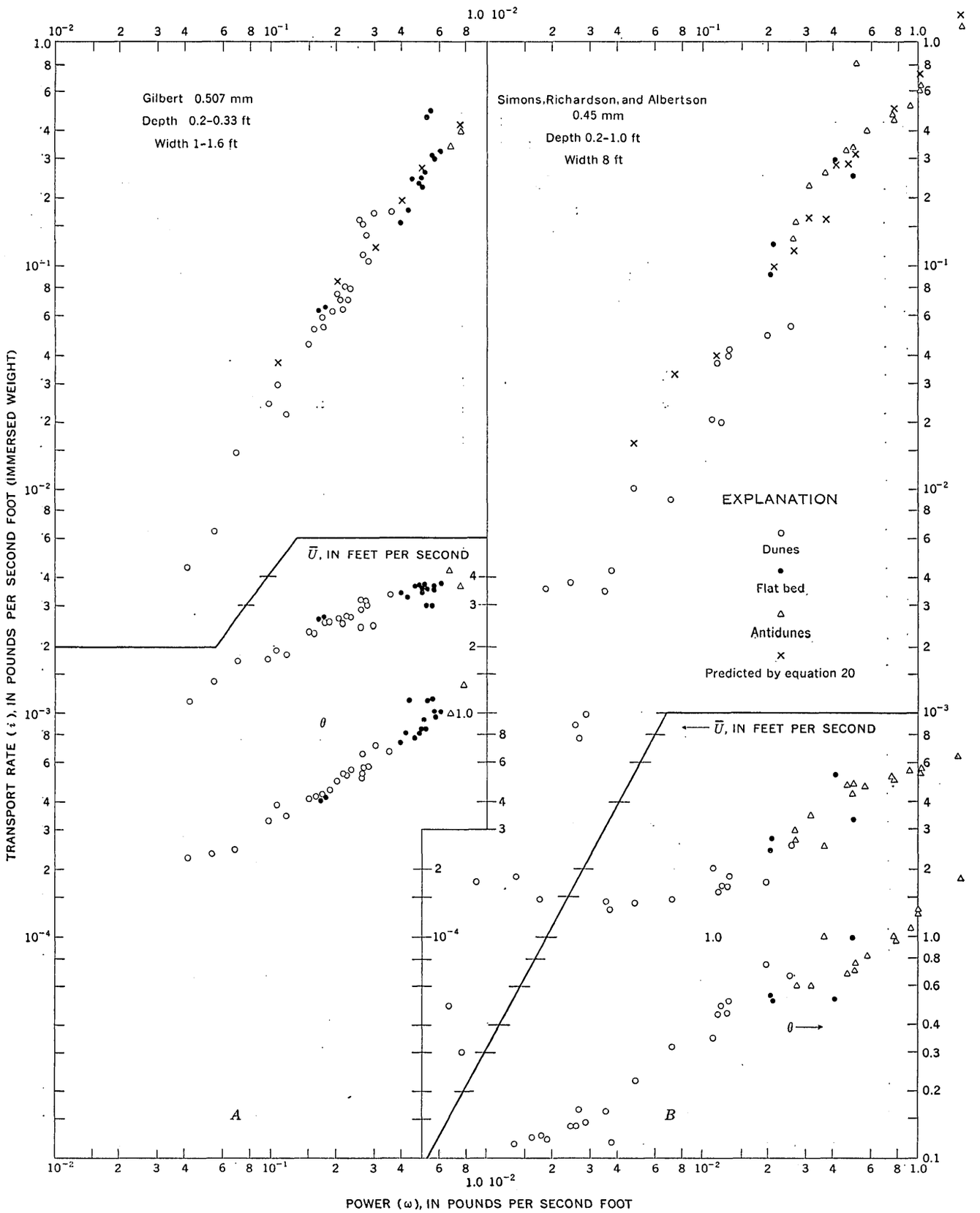

FIGURE 10.—Comparative plots of theoretical and experimental transport rates (flume experiments). *A*, Gilbert 0.507-mm sand. *B*, Simons, Richardson, and Albertson 0.45-mm sand.

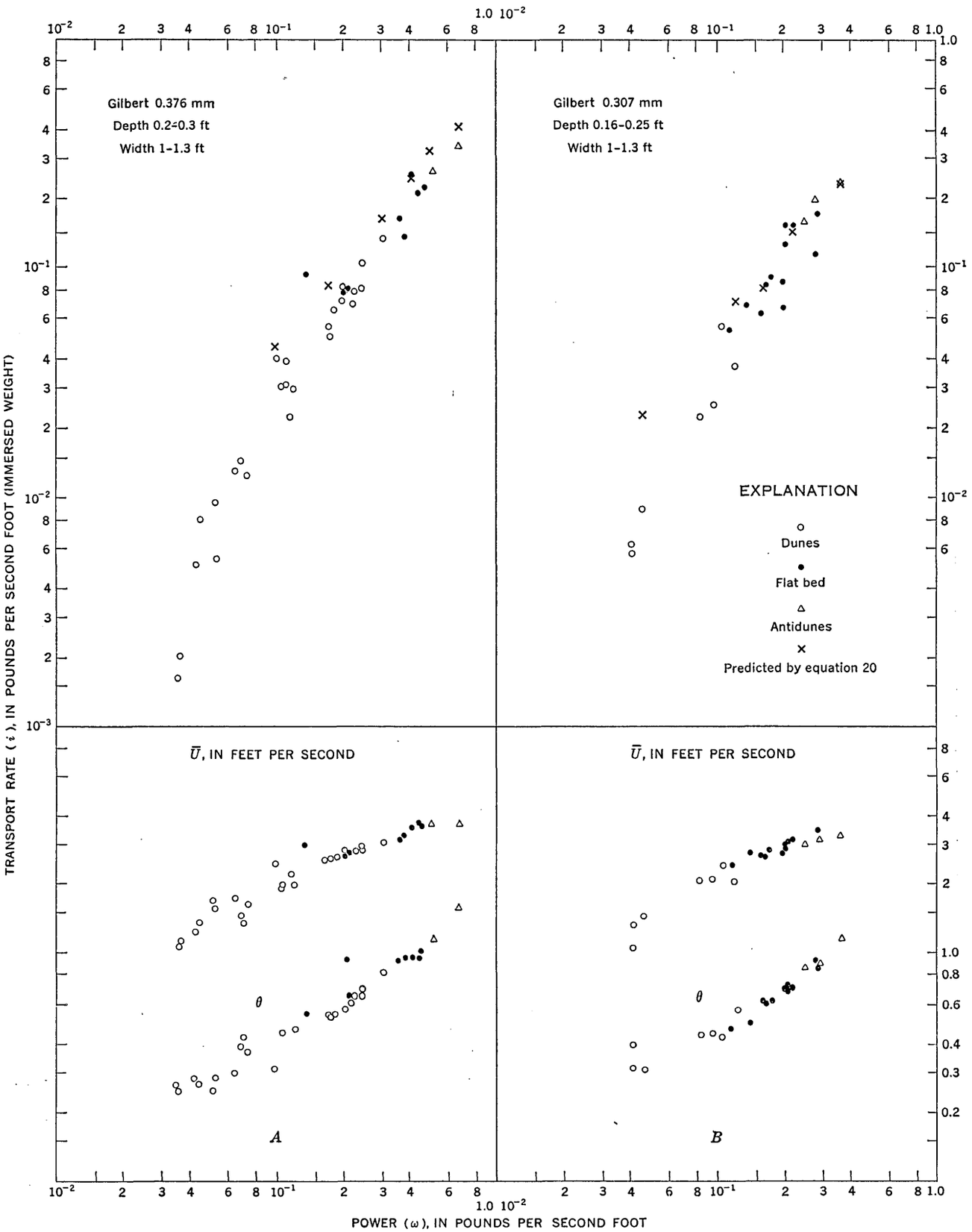

FIGURE 11.—Comparative plots of theoretical and experimental transport rates (flume experiments). *A*, Gilbert 0.376-mm sand. *B*, Gilbert 0.307-mm sand.

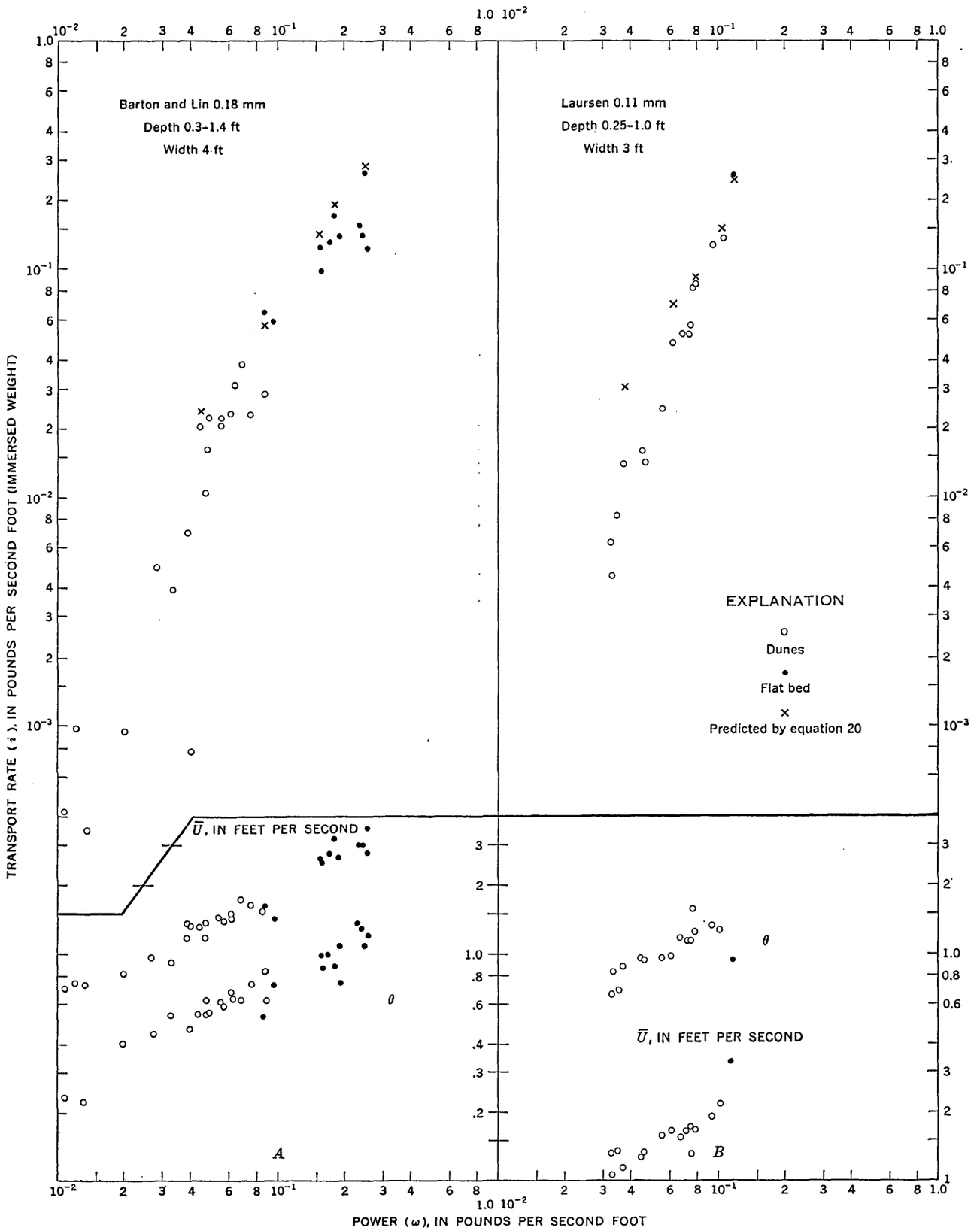

FIGURE 12.—Comparative plots of theoretical and experimental transport rates (flume experiments). *A*, Barton and Lin 0.18-mm sand. *B*. Laursen 0.11-mm sand.

SIMONS, RICHARDSON, AND ALBERTSON (1961) 0.45-mm SAND

Figure 10*B*

Depth range 140 to 700 diameters. Adequate? No evident correlation with flow depth, in spite of the wide depth range. However, there is an unfortunately large uncorrelatable scatter. This is probably due to too infrequent measurements of the transport rate during the runs. The scatter is noticeably greater over the lower, transitional stages, when large long-period fluctuations in the discharge of solids from the flume are to be expected as alternate dunes and troughs pass the end of the flume. Significantly, the transport-rate measurements were made by periodic sampling at the immediate exit from the flume. Max $\theta=1.2$. $V=0.1$ ft per sec. Average ratio $i_s/i_b=2.2$ over the higher stages. Load ratio 0.4.

Critical stage: predicted from figure 4, $\theta=0.5$. From plot, flat beds, $\theta=$approx 0.5; change of trend, $\theta=$approx 0.5.

GILBERT (1914) 0.376-mm SAND

Figure 11*A*

Depth range 160 to 240 diameters. Max $\theta=1.5$. $V=0.086$ ft per sec. Average ratio $i_s/i_b=2.3$. Load ratio 0.42.

Critical stage: predicted $\theta=0.5$. From plot, flat beds, $\theta=$ approx 0.6; change of trend, θ between 0.5 and 0.6.

GILBERT (1914) 0.307-mm SAND

Figure 11*B*

Depth range 200 to 300 diameters. Max $\theta=1.1$. $V=0.066$ ft per sec. Average ratio $i_s/i_b=2.6$. Load ratio 0.47.

Critical stage: predicted $\theta=0.5$. From plot, flat beds, θ between 0.5 and 0.6; change of trend, θ between 0.6 and 0.7.

BARTON AND LIN (1955) 0.18-mm SAND

Figure 12*A*

Depth range 500 to 2700 diameters. Max $\theta=1.4$. $V=0.035$ ft per sec. Average ratio $i_s/i_b=4.8$. Load ratio 0.86.

Critical stage: predicted $\theta=0.5$. From plot, flat beds, θ between 0.5 and 0.6; change of trend, θ between 0.5 and 0.7. Inexplicable scatter.

LAURSEN (1957) 0.11-mm SILT

Figure 12*B*

Max $\theta=1.6$. $V=0.0175$ ft per sec. Average ratio $i_s/i_b=6.1$. Load ratio 1.1.

Critical stage: predicted $\theta=0.5$. From plot, flat beds, value of θ uncertain; beginning of trend coincidence, θ between 1.1 and 1.4.

GENERAL COMMENTS

The mutual consistence between the experimental results is remarkable in view of the differences in the experimental conditions—different experimenters and methods of measurement, different apparatus from nonrecycling to recycling flumes, and different grain-size distributions.

There is also a surprising general agreement, all differences being within the limits of experimental error, between these results and those predicted by the present theory, over the 50-fold range of grain sizes covering nearly the whole range of transport modes from transport as bedload alone to transport in which suspension greatly predominates.

The scatter tends to obscure evidence of the critical stage at which the theory becomes operative. This stage appears to be predictable to a fair approximation by a critical value of the bedload criterion θ between 0.5 and 0.6 for Gilbert's data. But these data refer to narrow grain-size distribution. Other plots suggest that the critical stage occurs at considerably larger values of θ. However, this discrepancy may well be apparent rather than real. For with a wider size distribution the finer grades tend to be removed into suspension, leaving the bedload consisting of grades appreciably coarser than the mean stock size. Thus, were θ to be based, as it theoretically should be, on the mean bedload size, its value would be appreciably smaller. It would however be unwise to speculate further about this until experiment is improved toward repeatability by the avoidance of the scatter, and until methods are devised for measuring the size distribution of the grains in transit close over the bed.

Obviously a comprehensive investigation is needed to determine the causes of this unfortunate scatter, including the relative effects on the transport rate of (*a*) wall drag at various flow stages and for various grain sizes, and (*b*) the real effective height to which the bedload rises at high-flow stages.

Further, for more accurate application of the theory, it is evident that more attention should be paid to the size distributions of the suspended load, so that the effective value of V can be better estimated.

With regard to the scatter, the plots show that it is far narrower in the predicted transport-rate values than in the experimentally measured values. Since the predicted values are based on the same experimental values of the flow quantities ω and $\bar{u}$ and on a systematically estimated value of V, it follows that either there were large variations in the real effective value of V from run to run, which seems unlikely, or alternatively the experimental scatter originated in the measurement of the transport rates.

It is significant that the experimental scatter is worse, on the whole, for modern experiments done in recycling flumes, in which this measurement has to be by sampling, than for Gilbert's experiments done in a nonrecycling flume, in which the transport-rate measurement was direct, by integrated weight.

However accurately the sampling method may measure the instantaneous discharge of solids, it cannot make accurate measurement of the mean value of a spontaneously fluctuating discharge unless samples are taken systematically over a period covering several fluctuations.

EXPERIMENTS BY VANONI, BROOKS, AND NOMICOS

That the scatter which mars most of the experimental results can be greatly reduced by proper experimental design is shown in figures 13 *A* and *B* by the results of experiments carried out at California Institute of Technology (Brooks, 1957).

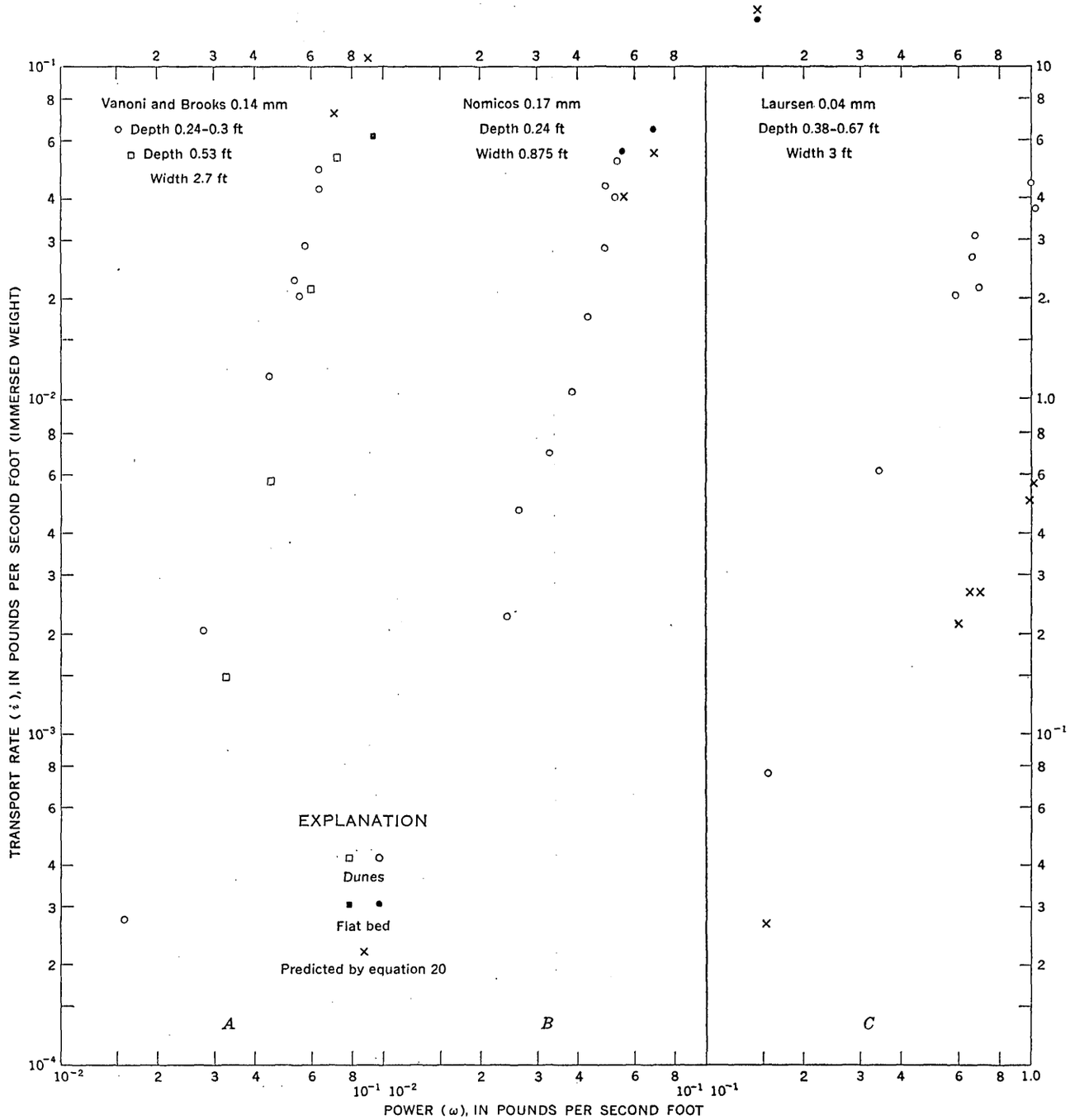

FIGURE 13.—Comparative plots of theoretical and experimental transport rates (flume experiments). *A*, Vanoni and Brooks 0.14-mm sand, *B*, Nomicos 0.172-mm sand, *C*, Laursen 0.04-mm silt.

These experiments differ from all others in that efforts were made to maintain constant flow depth, that is, to vary the tractive conditions alone, without varying the boundary conditions simultaneously.

Figure 13*A* shows the measured transport rates of the same sand, $D_{50\ \text{percent}}=0.14$ mm, at two different flow depths of approximately 0.24 and 0.54 feet in the same recycling and tilting flume 2.8 feet wide.

Though each of the two superimposed plots is highly consistent within itself, there is a systematic discrepancy between them. This discrepancy emphasizes the need to find out by well-designed and critical experiment the answers to the following questions: Is the discrepancy due to differences in relative wall drag; or is it due to excessive transport of bedload at the smaller depth, this depth supposedly being inadequate in the sense already discussed; or is it inherent in the arbitrary method of estimating the mean flow depth, as a factor of ω, over a rippled and highly irregular flow boundary; or is it perhaps a combination of all three?

In figure 13*B* are plotted the transport rates of another sand of considerably wider size distribution, $D_a=0.172$ mm, measured by Nomicos in a narrower flume but 0.875 feet wide. The flow depth was kept at 0.24 feet.

The results are again consistent, and this consistency discloses a clearer picture than before of the abrupt change of trend which occurs at the critical stage.

Superimposed are the theoretical transport rates calculated from equation 20 on the same arbitrary assumption as before that the effective suspension fall velocity $V=\frac{1}{2}\Sigma pV_p$ where the summation is taken over the given size distribution for the whole stock of material.

RELATION BETWEEN i AND ω OVER THE LOWER, TRANSITIONAL STAGES

It is not the purpose of this paper to consider conconditions over the lower, transitional stages between the threshold of motion and the critical stage. The very marked linearity of the logarithmic plots in this region is nevertheless noteworthy. It appears in all the relevant plots in which transport by suspension predominates: figures 10*B*, 12*A*, 12*B*, 13*A*, and 13*B*. It is particularly striking in the last two figures.

The transport rate i increases as ω^n, where the mean value of n approximates 3. I offer no explanation.

TRANSPORT OF FINE SILTS IN EXPERIMENTAL FLUMES

Laursen repeated his own experiments on the 0.11-mm sand, using a still finer material having a mean size of 0.038 mm. The measured transport rates are plotted in figure 13*C* together with the theoretical rates given by equation 20 on the same standard assumption that $V=\frac{1}{2}\Sigma pV_p$ over the size distribution of the stock material. On this basis $V=0.0047$ ft per sec, corresponding to a uniform $DV=0.04$ mm.

As can be seen, the measured rates are too large by an order of 10, and this might at first be taken to indicate the breakdown of the theory. A study of the report, however, suggests that such an anomaly is rather to be expected in view of the particular experimental conditions.

The solids enter a recycling flume more or less uniformly dispersed throughout the flow depth. The coarser grades fall to the neighborhood of the bed, where under normal experimental conditions they are transported along the bed as bedload. At the exit they are remixed with the circulating load.

However, at the high transport concentrations prevailing for fine materials having a small fall velocity V—concentrations approaching 10 percent in Laursen's experiments—the bed boundary is invisible. So the flow has to be stopped to allow the suspension to settle out before depth measurements can be made.

This deposition had the reported effect of blanketing the bed to the extent that the ripple features were partly obliterated. As a result, it seems reasonable to suppose, the subsequent transport of the coarser bed grains being prevented, the circulating load would become progressively finer as the coarser constituents were progressively trapped. (It is significant that deposition over the first 70 ft of the flume was reported to be continuing while transport measurements were made over the final 20 ft.)

No analysis, unfortunately, appears to have been made of the size constitution of the circulating load. It may well have consisted mainly of the 15 percent of the bed stock which was less than 0.02 mm in size, for which the effective fall velocity V would be of the order of 0.0007 ft per sec.

The flow velocities being around 2 ft per sec, this value of V inserted into equation 20 would give predicted transport rates of the same order as those measured.

The theory does indeed become inapplicable when the effective grain size is reduced below, say, 0.015 mm, as is evident from considerations of spatial concentration. Two-phase flow at very high concentrations is beyond the scope of the present paper. It has already been discussed in previous papers (Bagnold, 1954, 1955, 1956).

THE AVAILABLE RIVER DATA, NATURE, AND UNCERTAINTIES

The considered river data consist of 146 sets of records taken on various dates at various stations on certain rivers in western conterminous United States by the U.S. Geological Survey. These sets were selected some years ago by L. B. Leopold, before the present theory had been conceived, as being most likely to be reasonably reliable.

Each set comprises the flow data, the transport rate measured by sampling the flow, and integrated size analyses both of the sampled solids transported and of samples taken simultaneously from the bed surface.

The factual information is in this respect more complete and more readily comparable with the theory than is the experimental evidence. Further, both the width to depth ratios and the flow depths are much larger; so the uncertainties arising from the influence of side boundaries, from the likelihood of inadequate flow depth, and from Froude number disturbances are absent or greatly reduced.

There are, on the other hand, a number of other uncertainties.

ENERGY-SLOPE ESTIMATION

In many sets of data all reference to slopes was omitted from the original records. So the necessary information had to be obtained subsequently from map contours. Provided no discontinuities of profile at local rapids have been overlooked, and provided the river flow is not artificially constricted locally—for example, by bridge works—this map slope may be assumed to coincide with the true-energy slope at bankfull or flood stage.

In other data sets the recorded slope is the directly measured slope of the local water surface. Comparison with the map slope shows that in general the slope of the local water surface may be smaller at low river stages by a factor of 2 or more, owing to local irregularities of bed profile.

Only at one station have the true energy slopes been computed from measurements of both water surface and bed profiles. Naturally such costly and time-consuming measurements are unlikely to be made unless a need for them is clearly established.

BEDLOAD AND SUSPENDED LOAD

Unlike flume experiments in which it is possible to measure the total transport rates directly, the transport rates obtained for rivers are derived from samples taken from the body of the flow, integrated over the cross section. So there is an indeterminate deficiency in respect to the unsampled transport passing close over the bed.

This unmeasured transport is often referred to loosely as that of "bedload." Since, however, the magnitude of it depends entirely on the inadequacy of the humanly devised method of measurement, it is unrelated to the magnitude of the real bedload transport as defined by its dynamic mechanism.

As already pointed out, the maximum height above the bed to which the real bedload may rise, at high flow stages, is not known. So how much of it may have been included in the sampling and how much excluded cannot be determined. It is known for instance that by placing large-scale obstacles on a riverbed the local turbulence is increased to the extent that a large proportion of the normal bedload is thrown up into temporary suspension and can thus be included in the sampling. Since at high river stages the bed is frequently invisible, there may be undetected obstacles upstream doing the same thing.

In face of this uncertainty I have had to assume, as an arbitrary systematic assumption, that the real and fictitious bedloads are the same. Consequently, the recorded transport rates are assumed to refer to the suspended load alone. Consistently, the comparable predicted rates have been computed from equation 20 using only the second, suspension term $0.01\ \bar{u}/V$.

Since the first, bedload term $e_b/\tan\alpha$ is nearly constant at around 0.18, the effect of ignoring the bedload becomes serious only when the suspension term is of the same small order. The error may then mount to a factor of, say, 1.5 either way. The suspension term in many data sets is, however, much larger.

The above assumption also introduced possibly more serious error. The effective fall velocity $V=\Sigma pV_p$ is computed directly from the recorded size distribution on the assumption that this refers to the suspended load. But the undetected inclusion of even a small proportion, say 5 percent only, of the coarser bedload may so alter the pattern of the size distribtuion as to have a profound effect on the computed value of V. The value of V would be too large, and the predicted transport rate may in consequence be several times too small. As can be seen from the sample computations of V given earlier, the summation is very sensitive to small changes in the proportions of the few largest grades.

DEFICIENCY OF SEDIMENT SUPPLY

It may well happen, on the other hand—for example, after a flood stage has removed much of the transportable material from the riverbed—that the river transports less sediment than it could if more transportable

sediment were available. The predicted rates might then be considerably larger than the actual measured rates.

VALUES OF THE STAGE CRITERION θ

The size analysis of the bed surface being given, θ should be capable of direct determination from it by putting $D=D_a=\Sigma pD_p$. However, some uncertainty arises from the fact that, again unlike laboratory conditions, the largest bed grains according to the analyses are often greater by a factor of 30 or more than the largest transported grains. So it is open to some doubt whether or not the whole bed surface can be assumed to be mobile.

Again, though the value of θ is an approximate guide in default of a better one, it is not, as pointed out earlier, a precise criterion for either the disappearance of dune features on the bed or the change of trend in the transport rate versus power curves. As is apparent from figures 9 to 11, dune features often persist at the higher flow stages where the theory agrees with the data. Accordingly agreement with the river data is found even when dunes are known to be present.

In view of these various uncertainties, many discrepancies, in both directions, must be expected when comparing the predicted with the measured transport rate.

COMPARISON OF PREDICTED WITH MEASURED RIVER TRANSPORT RATES

In contrast to laboratory conditions, in which the same stock of sediment material taken from some natural deposit of limited size distribution is transported at progressively increasing flow stages, the material transported by a river, together with that of the local bed surface, changes from season to season, from day to day, and often from hour to hour, according to the ever-changing tributary influxes upstream.

A group of records taken at the same gaging station on different dates would therefore show little if any correlation. So it would be unprofitable to plot the transport rates. Instead, each record should be treated as though it were the result of a separate and independent experiment done on the transport of a different sediment stock.

Accordingly I have tabulated the river records (table 1) so as to compare the transport rates measured on each separate occasion with the rate predicted for that occasion from the flow and sediment conditions then prevailing.

TABLE 1.—*Data from 146 individual river measurements comparing measured with predicted transport rates*

[Slope: M, map slope; L, measured slope of local water surface; ES, estimated true-energy slope. Basic data compiled by L. B. Leopold from various sources, mostly measurements by U.S. Geol. Survey. The compilation included arbitrarily chosen individual measurements to illustrate conditions over a range of discharges. Measurement stations in the tabulation were limited to those for which complete discharge and suspended-load data were available. Data are available in the files of the U.S. Geol. Survey, Washington, D.C.]

Date	USGS serial No.	Discharge (cfs) Q	Depth (feet) d	Slope S	Mean velocity (ft per sec) $\bar{u}$	Bed: Grain size (mm) Maximum D	Bed: Grain size (mm) Mean D_a	Bed shear stress θ	Suspended load: Fall velocity $V=\Sigma pV_p$ (cm per sec)	Suspended load: Concentration C	Transport rate: Measured $\frac{C'}{S}=\frac{i_s}{\omega}$	Transport rate: Predicted $\frac{i_s}{\omega}=0.01\frac{\bar{U}}{V}$	Transport rate: Discrepancy predicted/measured
BRAZOS RIVER													
Richmond, Tex.													
5- 7-57	1	107,000	28.2	1.59×10⁻⁴ (M)	6.83	>16	0.4		0.72	2.24×10⁻³	8.75	2.9	0.33
4- 3-57	2	3,460	9.5	1.59×10⁻⁴ (M)	2.83	16	.24	1.1	.083	3.88×10⁻³	15.2	10.0	.66
5-14-57	3	59,000	26.5	1.59×10⁻⁴ (M)	4.7	8	.9	.91	.159	3.0 ×10⁻³	11.7	8.9	.76
5- 9-58	4	31,000	18.8	1.59×10⁻⁴ (M)	3.96	16	1.9	.2	.24	3.19×10⁻³	12.5	5.0	.42
4-24-57	5	31,760	14.9	1.59×10⁻⁴ (M)	5.47	4	.36	1.4	.122	6.76×10⁻³	26.4	13,5	.51
10-18-57	6	83,600	27.5	1.59×10⁻⁴ (M)	6.3				.215	7.07×10⁻³	24.8	9.0	.36
10-24-57	7	51,300	23.3	1.59×10⁻⁴ (M)	5.0	16		.7	.175	4.24×10⁻³	16.5	8.9	.54
COLORADO RIVER (OF THE WEST) [1]													
Taylors Ferry, Ariz.													
5- 2-56	248	7,900	8.57	1.73×10⁻⁴ (L)	2.63	2	0.4	0.7	1.75	7.6 ×10⁻⁵	0.27	0.45	1.67
9- 6-56	218	9,880	9.41	1.47×10⁻⁴ (L)	2.99	8	.64	.4	1.75	1.18×10⁻⁴	.5	.515	1.03
9-20-56	219	6,625	7.45	1.73×10⁻⁴ (L)	2.55	4	.8	.3	2.83	2.07×10⁻⁴	.72	.44	.61
10- 5-56	220	6,400	7.38	1.78×10⁻⁴ (L)	2.49	2	.45	.55	1.17	2.69×10⁻⁴	.935	.675	.68
9-15-55	208	10,845	9.9	2.16×10⁻⁴ (L)	3.08	2	.35	1.15	1.73	1.59×10⁻⁴	.45	.53	1.16
12-15-55	209	4,200	4.92	3.3 ×10⁻⁴ (L)	2.49	1	.31	1.0	2.0	9.4 ×10⁻⁵	1.75	.37	.21
12-29-55	210	4,760	5.4	2.6 ×10⁻⁴ (L)	2.53	1	.17	1.5	1.96	1.4 ×10⁻⁴	.33	.39	1.17
3- 5-56	211	7,762	7.02	1.9 ×10⁻⁴ (L)	3.17	2	.2	1.25	1.78	1.16×10⁻⁴	.38	.53	1.4
3-21-56	212	7,767	7.7	2.16×10⁻⁴ (L)	2.89	2	.19	1.65	1.93	1.51×10⁻⁴	.43	.45	1.05
4- 3-56	213	10,733	9.81	2.07×10⁻⁴ (L)	3.12	2	.37	1.03	1.44	2.44×10⁻⁴	.73	.64	.88
	214	9,533	9.25	2.24×10⁻⁴ (L)	2.93	1	.19	2.04	2.1	9.39×10⁻⁵	.26	.42	1.6
5-17-56	215	7,409	7.67	2.27×10⁻⁴ (L)	2.76	4	.36	.9	2.26	1.51×10⁻⁴	.38	.37	.96
5-31-56	216	8,480	7.61	1.87×10⁻⁴ (L)	3.17	16	1.2	.215	1.77	7.7×10⁻⁵	.255	.88	[2] 4.1
8-21-56	217	10,480	9.7	2.33×10⁻⁴ (L)	3.08	2	.5	.85	1.66	5.0 ×10⁻⁵	.13	.57	4.4

See footnotes at end of table.

TABLE 1.—*Data from 146 individual river measurements comparing measured with predicted transport rates*—Continued

Date	USGS serial No.	Discharge (cfs) Q	Depth (feet) d	Slope S	Mean velocity (ft per sec) u	Bed: Grain size (mm) Maximum D	Bed: Grain size (mm) Mean D_a	Bed shear stress θ	Suspended load: Fall velocity $V=\Sigma p V_p$ (cm per sec)	Suspended load: Concentration C	Transport rate: Measured $\frac{C'}{S}=\frac{i_s}{\omega}$	Transport rate: Predicted $\frac{i_s}{\omega}=0.01\frac{\bar{U}}{\bar{V}}$	Transport rate: Discrepancy predicted/measured
COLORADO RIVER (OF THE WEST)—Continued													
Below Needles, Ariz.													
10-17-56	239	8,600	8.61	1.77×10^{-4} (L)	3.02	2	0.34	0.94	0.893	3.79×10^{-4}	1.32	0.67	0.51
7-31-56	240	10,365	10.77	1.53×10^{-4} (L)	2.86	16	.58	.53	1.89	1.13×10^{-4}	.455	.455	1.0
8-10-55	250	12,316	11.69	1.96×10^{-4} (L)	3.07	0.5	.3	1.46	2.94	1.1×10^{-4}	.35	.31	.89
9-30-55	251	12,670	11.86	2.2×10^{-4} (L)	3.17	1	.3	1.63	3.02	2.44×10^{-4}	.69	.5	.725
12- 8-55	252	3,855	5.24	2.77×10^{-4} (L)	2.44	1.5	1.0	.27	3.34	2.6×10^{-4}	.58	.22	.38
1- 5-56	253	7,024	7.73	2.77×10^{-4} (L)	2.81	2	.25	1.6	2.48	1.92×10^{-4}	.43	.34	.79
3- 7-56	254	7,780	10.0	2.13×10^{-4} (L)	2.3	3	.3	1.3	1.8	1.52×10^{-4}	.44	.38	.86
4-13-56	255	10,357	10.88	1.93×10^{-4} (L)	2.75	8	.35	1.15	3.71	4.7×10^{-4}	1.55	.31	.2
Lees Ferry, Ariz.													
10-16-55	----------	3,560	4.3	2.23×10^{-3}(M)	2.47	1	0.20	9	0.265	1.01×10^{-3}	0.27	2.8	10
6- 3-56	----------	62,000	18.1	2.23×10^{-3}(M)	8.95	1	.32	23	1.37	6.25×10^{-3}	1.74	1.97	1.13
6-25-58	----------	33,100	16.6	2.23×10^{-3}(M)	5.21	1	.21	30	.48	1.8×10^{-3}	.5	3.24	6.48
4-14-56	----------	10,000	7.73	2.23×10^{-3}(M)	3.55	6	.33	11	.52	3.0×10^{-3}	.835	2.04	2.45
Grand Canyon, Ariz.													
4-12-56	C	11,300	9.73	1.89×10^{-3}(M)	4.08	0.9	0.34	10	0.25	4.57×10^{-3}	1.5	4.9	3.25
5-31-56	K	54,300	20.1	1.89×10^{-3}(M)	9.02	4.0	.45	16	1.19	9.0×10^{-3}	2.95	2.27	.77
5-17-55	F	27,110	14.6	1.89×10^{-3}(M)	6.29	.5	.2	27	.7	8.88×10^{-3}	2.9	2.7	1.06
Palo Verde Weir, Ariz. (1.4 miles below)													
5-31-56	203	12,180	9.2	1.6×10^{-4}(L)	2.87	16	1.2	0.23	2.86	9.27×10^{-5}	0.35	0.30	0.85
5- 2-56	201	12,170	8.9	1.13×10^{-4}(L)	2.98	16	1.3	.14	2.11	1.09×10^{-4}	.64	.43	.66
5-17-56	202	10,660	8.67	1.47×10^{-4}(L)	2.78	>16	----------	----------	2.98	2.14×10^{-4}	.9	.29	.32
8-21-55	204	11,860	9.74	6.0×10^{-5}(L)	2.64	>16	----------	----------	3.6	2.06×10^{-4}	.97	.70	.73
9- 6-56	205	9,880	8.95	1.53×10^{-4}(L)	2.41	16	1.6	.17	1.55	1.42×10^{-4}	.65	.48	.74
9-26-56	206	10,200	8.8	6.6×10^{-5}(L)	2.58	3	0.28	.57	1.43	1.46×10^{-4}	1.38	.54	.39
10- 5-56	207	8,440	8.25	1.27×10^{-4}(L)	2.31	4	.22	.9	1.03	2.69×10^{-4}	1.3	.69	.53
9-16-55	241	9,461	9.93	5.3×10^{-5}(L)	2.93	8	2.2	.05?	1.6	7.1×10^{-5}	.83	.55	.66
12-14-55	242	4,412	6.87	1.06×10^{-4}(L)	2.04	8	.63	.2	2.0	5.2×10^{-5}	.3	.3	1
12-28-55	243	4,174	6.9	1.13×10^{-4}(L)	1.93	8	.86	.17	2.75	1.12×10^{-5}	.062	.2	3.2
3- 6-56	244	6,778	7.74	1.4×10^{-4}(L)	2.66	>16	1.5	.14	2.1	1.29×10^{-4}	.58	.38	.65
3-21-56	245	9,633	9.25	1.03×10^{-4}(L)	3.08	>16	----------	----------	6.47	1.68×10^{-4}	1.0	.14	.14
4- 2-56	246	12,819	10.87	1.27×10^{-4}(L)	3.27	>16	----------	----------	2.85	1.69×10^{-4}	.84	.35	.42
4-19-56	247	10,900	9.00	1.2×10^{-4}(L)	2.75	>16	----------	----------	1.76	6.3×10^{-5}	.32	.47	1.46
COLORADO RIVER (OF TEXAS)													
Columbus, Tex.													
4- 2-57	8	2,250	5.06	2.3×10^{-4}(M)	2.04	2	0.36	0.62	0.030	1.57×10^{-3}	4.25	20	4.7
5- 9-57	9	13,000	11.34	2.3×10^{-4}(M)	2.54	16	1.17	.4	.23	4.48×10^{-4}	1.2	3.3	2.7
9-26-57	10	16,100	21.7	2.3×10^{-4}(M)	5.34	8	.5	1.9	.92	1.94×10^{-3}	5.2	1.7	.33
4- 9-59	11	8,500	6.8	2.3×10^{-4}(M)	2.93	1	.3	.98	.89	1.68×10^{-3}	4.55	1.0	.22
9-25-57	12	4,600	4.5	2.3×10^{-4}(M)	2.48	2	.35	.55	.08	1.97×10^{-3}	5.3	9.3	1.75
5- 6-57	13	31,800	16.18	2.3×10^{-4}(M)	3.93	12	.55	1.25	.59	6.87×10^{-4}	1.85	2.0	1.08
9-22-58	14	24,600	11.2	2.3×10^{-4}(M)	4.57	1	.34	1.4	.2	2.62×10^{-3}	7.0	6.8	.98
10-17-57	15	36,700	18.2	2.3×10^{-4}(M)	3.95	16	1.5	.52	.15	2.57×10^{-3}	6.9	5.9	.86
9-25-57	16	18,500	10.1	2.3×10^{-4}(M)	4.12	.5	.24	1.8	.83	5.25×10^{-3}	14.2	1.5	.104
5- 4-58	17	2,460	13.0	2.3×10^{-4}(M)	3.37	8	.36	1.6	.41	2.34×10^{-3}	6.2	2.4	.39
4-27-57	18	31,550	12.86	2.3×10^{-4}(M)	5.0	1	.3	1.85	1.0	4.38×10^{-3}	12.8	1.5	.12
ELKHORN RIVER													
Near Waterloo, Nebr.													
3-26-52	257	2,830	3.07	4.03×10^{-4} (ES)	3.79	0.5	0.075	----------	0.68	3.43×10^{-3}	5.25	1.7	0.32
4- 1-52	258	8,850	6.08	3.7×10^{-4} (ES)	5.51	----------	----------	----------	.48	6×10^{-3}	10.0	3.4	.34
4- 2-52	259	7,860	5.73	4.33×10^{-4} (ES)	5.23	----------	----------	----------	.48	5.01×10^{-3}	7.2	3.3	.45
4- 3-52	260	6,520	5.46	4.75×10^{-4} (ES)	4.55	----------	----------	----------	.46	4.14×10^{-3}	5.4	3.0	.55
4-18-52	261	2,860	2.9	3.72×10^{-4} (ES)	3.68	----------	----------	----------	.59	1.52×10^{-3}	2.5	1.86	.75
5- 1-52	262	2,150	3.02	4.07×10^{-4} (ES)	2.78	----------	----------	----------	.65	1×10^{-3}	.95	1.27	1.34
5-15-52	263	1,500	2.84	4.38×10^{-4} (ES)	2.08	----------	----------	----------	.62	6×10^{-4}	.85	1.0	1.18
5-21-52	264	1,500	2.84	4.24×10^{-4} (ES)	2.14	----------	----------	----------	.43	6.98×10^{-4}	1.02	1.53	1.5
6-30-52	265	1,820	3.44	3.64×10^{-4} (ES)	2.05	----------	----------	----------	.08	3.41×10^{-3}	5.8	7.5	1.3
6-26-52	266	6,960	4.38	4.67×10^{-4} (ES)	6.00	2	.29	1.33	.18	2.1×10^{-2}	28.0	10.0	.36
7- 2-59	267	2,722	3.92	2.68×10^{-4} (ES)	3.02	1	.21	.93	.12	3.7×10^{-3}	8.6	7.6	.88
7- 2-59	268	2,272	4.0	2.68×10^{-4} (ES)	2.43	----------	----------	----------	.087	3.42×10^{-3}	7.9	8.4	1.06
7- 2-59	269	2,387	3.74	2.68×10^{-4} (ES)	2.77	8	1.2	.15	.086	3.3×10^{-3}	7.2	9.6	1.33
7- 2-59	270	2,387	3.8	2.68×10^{-4} (ES)	2.26	----------	----------	----------	.086	3.28×10^{-3}	4.75	7.9	1.65
7- 2-59	271	2,240	3.7	2.52×10^{-4} (ES)	2.64	1	.21	.83	.0855	3.41×10^{-3}	8.4	9.4	1.12
7- 2-59	272	2,240	3.78	2.52×10^{-4} (ES)	2.13	----------	----------	----------	.079	3.08×10^{-3}	7.6	8.1	1.07

See footnotes at end of table.

TABLE 1.—*Data from 146 individual river measurements comparing measured with predicted transport rates*—Continued

Date	USGS serial No.	Discharge (cfs) Q	Depth (feet) d	Slope S	Mean velocity (ft per sec) $\bar{u}$	Bed: Grain size (mm) Maximum D	Bed: Grain size (mm) Mean D_a	Bed shear stress θ	Suspended load: Fall velocity $V=\Sigma p V_p$ (cm per sec)	Suspended load: Concentration C	Transport rate: Measured $\frac{C'}{S}=\frac{i_s}{\omega}$	Transport rate: Predicted $\frac{i_s}{\omega}=0.01\frac{\bar{U}}{V}$	Transport rate: Discrepancy predicted/measured
GALISTEO CREEK													
Domingo, N. Mex.													
	F	448	0.71	4.44×10^{-3} (M)	4.23	16	1.2	0.49	0.2	1.1×10^{-1}	15.4	6.3	0.41
	E	381	.77	4.44×10^{-3} (M)	4.74	8	.62	1.05	.11	7.0×10^{-2}	9.8	12.9	1.31
RIO GRANDE													
Bernalillo, N. Mex.													
4-25-52	65	2,820	2.94	9.0×10^{-4} (L)	4.14	16	0.32	1.4	0.72	3.32×10^{-3}	2.3	1.73	0.75
4-25-52	66	2,820	1.18	1.03×10^{-3} (L)	3.72	12	.4	.55	.84	2.82×10^{-3}	1.7	1.32	.77
5-12-52	67	6,440	3.55	9.6×10^{-4} (L)	6.52	12	.6	1.1	1.38	3.71×10^{-3}	2.38	1.42	.6
5-12-52	68	6,440	2.09	8.8×10^{-4} (L)	5.4	12	.6	.58	.94	2.84×10^{-3}	2.0	1.72	.86
6-17-52	69	6,120	3.72	8.6×10^{-4} (L)	5.95	12	.38	1.6	2.21	2.36×10^{-3}	1.7	.81	.47
6-17-52	70	6,120	2.18	7.5×10^{-4} (L)	5.73	8	.45	.68	1.45	1.75×10^{-3}	1.45	1.18	.81
6-20-52	71	4,775	3.44	8.4×10^{-4} (L)	5.04	16	.62	.88	1.7	1.66×10^{-3}	1.23	.89	.72
6-20-52	72	4,775	2.51	8.6×10^{-4} (L)	5.43	12	.48	.84	1.77	1.57×10^{-3}	1.13	.92	.82
6-26-52	73	2,800	2.75	7.9×10^{-4} (L)	3.74	8	.40	1.0	1.86	9.42×10^{-4}	.74	.6	.81
6-26-52	74	2,800	2.42	1×10^{-3} (L)	3.11	16	.73	.65	1.35	9.46×10^{-4}	.58	.69	1.2
7-24-52	75	2,030	2.69	9.6×10^{-4} (L)	2.77	8	.36	1.35	.58	2.74×10^{-3}	1.77	1.43	.81
7-24-52	76	2,030	1.58	9.3×10^{-4} (L)	2.2	12	.53	.52	.5	1.94×10^{-3}	1.29	1.32	1.02
6-18-58	77	4,000	2.76	1.14×10^{-3} (L)	5.06				1.67	5.98×10^{-3}	3.26	.91	.28
6-13-58	78	4,340	2.67	1.15×10^{-3} (L)	6.10	12	.54	1.07	1.53	2.08×10^{-3}	1.12	1.2	1.07
6-10-58	79	5,800	3.43	1.2×10^{-3} (L)	6.27	16	0.62	1.25	2.87	3.48×10^{-3}	1.8	0.65	0.37
6-25-58	80	6,040	3.40	1.2×10^{-3} (L)	6.5	12	0.44	1.6	2.77	5.41×10^{-3}	2.8	.71	.25
5- 8-58	81	6,860	3.68	1.27×10^{-3} (L)	6.91	16	.86	1.02	1.16	4.42×10^{-3}	2.16	1.78	.83
6- 4-58	82	8,160	4.34	1.15×10^{-3} (L)	6.92	1	.32	2.8	1.64	2.58×10^{-3}	1.4	1.26	.9
5-13-58	83	8,320	4.46	1.27×10^{-3} (L)	6.88	12	.48	2.2	1.21	4.74×10^{-3}	2.3	1.73	.75
5-27-58	84	10,100	4.8	1.2×10^{-3} (L)	7.71	12	.41	2.6	1.39	3.04×10^{-3}	1.57	1.66	1.06
San Antonio, N. Mex.													
6-26-58	85	378	1.21	[3] 4.5×10^{-4} (L)	1.58	8	0.30	0.34	.97	9.04×10^{-4}	1.24	0.48	0.39 ([4] .68)
6-19-58	86	3,080	2.59	[3] 3.5×10^{-4} (L)	5.24	.5	.173	1.0	.6	5.38×10^{-3}	9.4	2.6	.28 ([4] .63)
6- 9-58	87	4,090	3.28	[3] 5.0×10^{-4} (L)	5.44	8	.30	1.02	.72	4.62×10^{-3}	5.7	2.26	.4 ([4] .63)
6-11-58	88	4,260	3.26	[3] 6.0×10^{-4} (L)	5.66	1	.24	1.5	.71	4.56×10^{-3}	4.7	2.4	.51 ([4] .67)
5- 8-58	89	6,180	3.87	[3] 5.5×10^{-4} (L)	6.79	1	.69	.58	.61	1.26×10^{-2}	14.1	3.3	.24 ([4] .34)
6- 5-58	90	6,570	4.23	[3] 5.5×10^{-4} (L)	6.61	1	.22	2.0	2.15	6.07×10^{-3}	6.85	.92	.13 ([4] .18)
5-29-58	91	8,500	4.98	[3] 5.5×10^{-4} (L)	7.26	4	.25	2.1	.8	7.61×10^{-3}	8.6	2.72	.32 ([4] .46)
6-19-52	92	4,850	3.17	7.9×10^{-4} (M)	5.89	8	.27	1.74	.83	3.8×10^{-3}	3.0	2.14	.71
5-13-58	102	6,940	4.29	[5] 6.5×10^{-4} (L)	6.81	1	.14	3.72	.91	1.15×10^{-2}	11.0	2.24	.2 ([4] .24)
5-22-58	103	7,740	4.64	[5] 5.5×10^{-4} (L)	7.04	1	.21	2.3	.54	9.28×10^{-3}	10.4	3.9	.37 ([4] .53)
St. Marcial floodway, N. Mex.													
6-27-58	93	1,990	2.73	[5] 4.5×10^{-4} (L)	3.99	.5	0.115	2.0	.344	3.73×10^{-3}	5.1	3.5	0.68 ([4]0.95)
6-20-58	94	3,810	3.62	[5] 3.5×10^{-4} (L)	5.6	.5	.157	1.51	.36	4.21×10^{-3}	7.5	4.7	.62 ([4] 1.1)
6-10-58	95	4,230	4.07	[5] 6.0×10^{-4} (L)	5.59	.5	.156	2.9	.55	4.37×10^{-3}	4.5	3.1	.68 ([4] .71)
6-12-58	96	4,570	4.06	[5] 5.0×10^{-4} (L)	5.95	1	.25	1.53	.50	4.08×10^{-3}	5.1	3.6	.7 ([4] .88)
5- 8-58	97	6,170	4.97	[5] 5.0×10^{-4} (L)	6.43	1	.14	3.3	.36	9.6×10^{-3}	11.9	5.4	.45 ([4] .57)
5-12-58	98	6,420	5.03	[5] 3.0×10^{-4} (L)	6.62	1	.13	2.1	.3	7.83×10^{-3}	16.1	6.6	.41 ([4] .86)
6- 6-58	99	6,870	5.39	[5] 2.0×10^{-4} (L)	6.61	.5	.15	1.35	.51	5.95×10^{-3}	18.5	4.0	.22 ([4] .68)
5-22-58	100	7,710	6.23	[5] 4.0×10^{-4} (L)	6.48	.5	.16	2.9	.33	6.08×10^{-3}	9.4	5.9	.62 ([4] .98)
5-28-58	101	8,680	6.75	[5] 4.0×10^{-4} (L)	6.53	.5	.17	3.0	.38	5.45×10^{-3}	8.5	5.2	.61 ([4] .96)
Otowi, N. Mex.													
5-12-58	276	9,340	10.23	2.46×10^{-3} (L)	7.02	8	0.54	8.7	3.0	5.02×10^{-3}	1.26	0.7	0.55
5- 6-58	277	7,320	8.11	2.3×10^{-3} (L)	6.84	>16	2.13	1.65	2.37	7.44×10^{-3}	2.0	.87	.43
6- 3-58	278	8,590	8.96	2.4×10^{-3} (L)	7.1	>16	3.51	1.15	1.8	1.72×10^{-3}	.44	1.15	2.65
6-12-58	279	5,000	7.19	2.31×10^{-3} (L)	5.56	>16	2.3	1.35	2.7	1.11×10^{-3}	.3	.62	2.0
6-17-58	280	2,240	4.69	1.63×10^{-3} (L)	4.23	16	1.1	1.3	7.2	1.86×10^{-3}	.73	.17	.24
6-24-58	281	1,130	1.44	1.31×10^{-3} (L)	3.35	>>16	?	?	2.79	3.16×10^{-4}	.15	.36	2.4
5-26-58	282	10,100	10.21	2.35×10^{-3} (L)	7.08	>16	1.54	1.0	1.62	2.99×10^{-3}	.79	1.3	1.6
Cochita, N. Mex.													
6-24-58	283	1,000	1.71	1.18×10^{-3} (L)	2.23	8	2.1	0.18	1.18	2.47×10^{-4}	0.13	0.56	4.3
6-17-58	284	2,040	2.24	1.18×10^{-3} (L)	3.2	8	1.0	.5	5.4	5.24×10^{-3}	2.75	.18	.065
6-17-58	285	5,060	4.03	1.13×10^{-3} (L)	4.22	>16	2.3	.37	8.1	8.84×10^{-3}	4.9	.16	.032
6- 3-58	286	8,680	4.85	1.27×10^{-3} (L)	6.07	>16	3.5	.33	3.5	3.11×10^{-3}	1.5	.51	.34
5-12-58	287	8,900	4.09	1.2×10^{-3} (L)	6.64	>16	2.23	.42	1.34	4.55×10^{-3}	2.35	1.48	.63
5-20-58	288	8,920	4.34	1.2×10^{-3} (L)	6.51	>16	5.0	.2	1.33	3.11×10^{-3}	1.6	1.47	.92
5-26-58	289	9,810	4.39	1.27×10^{-3} (L)	6.68	>>16			2.0	3.11×10^{-3}	1.5	1.0	.66

See footnotes at end of table.

TABLE 1.—*Data from 146 individual river measurements comparing measured with predicted transport rates*—Continued

Date	USGS serial No.	Discharge (cfs) Q	Depth (feet) d	Slope S	Mean velocity (ft per sec) $\bar{u}$	Bed: Grain size (mm) Maximum D	Bed: Grain size (mm) Mean D_a	Bed shear stress θ	Suspended load: Fall velocity $V=\Sigma p V_p$ (cm per sec)	Suspended load: Concentration C	Transport rate: Measured $\frac{C'}{S}=\frac{i_s}{\omega}$	Transport rate: Predicted $\frac{i_s}{\omega}=0.01\frac{\bar{u}}{V}$	Transport rate: Discrepancy $\frac{\text{predicted}}{\text{measured}}$
RIO GRANDE—Continued San Filipe, N. Mex.													
6-24-58	290	1,020	2.17	1.0 ×10⁻³ (L)	2.6	>>16			1.33	5.77 ×10⁻⁴	0.36	0.59	1.6
6-17-58	291	2,200	2.73	9.1 ×10⁻⁴ (L)	4.44	16	1.27	0.36	2.66	1.1 ×10⁻³	.75	.5	.66
6-17-58	292	5,010	4.47	1.51×10⁻³ (L)	5.99	>>16			5.3	2.74 ×10⁻³	1.12	.29	.26
6- 9-58	293	5,120	4.49	1.51×10⁻³ (L)	6.06	16	1.0	1.3	6.5	6.3 ×10⁻³	2.6	.28	.11
5- 7-58	294	7,520	5.57	1.52×10⁻³ (L)	6.7	(6)	(6)	(6)	1.4	4.62 ×10⁻³	2.5	1.44	.58
5-12-58	295	8,200	5.56	1.76×10⁻³ (L)	7.19	>>16			2.9	4.41 ×10⁻³	1.55	.75	.48
6- 3-58	296	8,590	6.0	1.68×10⁻³ (L)	7.16	16	2.1	0.9	2.3	2.430×10⁻³	.9	.94	1.05
5-21-58	297	9,140	5.86	1.8 ×10⁻³ (L)	7.43	>>16			1.56	2.79 ×10⁻³	.96	1.4	1.4
5-26-58	298	9,720	6.17	1.93×10⁻³ (L)	7.53	>>16			1.53	2.58 ×10⁻³	1.15	1.46	1.3
RIO PUERCO Bernado, N. Mex.													
8-10-59	1	1,600	2.62	1.05×10⁻³(M)	6.58	1	0.29	1.8	0.20	1.41×10⁻¹	83	10	0.12
8-26-59	2	2,010	2.64	1.05×10⁻³(M)	7.31	2	.33	1.6	.22	1.65×10⁻¹	97	10	.10
11- 3-59	3	31.8	.97	1.05×10⁻³(M)	1.37	2	.24	.8	.0074	4.8 ×10⁻²	28.4	56	2
SAN JUAN RIVER Shiprock, N. Mex.													
5-31-51	275	6,120	5.49	4.1 ×10⁻⁴ (L)	6.3	(6)	(6)	(6)	1.9	2.07×10⁻³	3.12	1	0.32
SCHUYLKILL RIVER Philadelphia, Pa.													
9- 3-59	256	13,000	8.08	5.3 ×10⁻⁴ (L)	4.9	>>16	Stony		0.27	4.88×10⁻⁴	0.57	5.5	9.6

[1] Data from Colorado River (of the West) unpublished, from U.S. Bur. of Reclamation, on file in U.S. Geol. Survey, Washington, D.C.; locations shown on map published by the U.S. Inter-Agency Committee on Water Resources (1961).
[2] Below critical stage.
[3] Map slope is 7.9×10⁻⁴. Local pool?
[4] Discrepancy using map slope.
[5] Map slope is 6.3×10⁻⁴. Local pool.
[6] No bed.

The comparison is given in terms of the dimensionless ratio $C'/S=i_s/\omega$, where C' is the transport concentration by immersed weight and is assumed to refer to suspended load only.

The effective fall velocity $V=\Sigma pV_p$ is given in centimeters per second for easy reference to standard values such as those plotted in Report 12 of the U.S. Inter-Agency Committee on Water Resources (1958). The predicted ratios $i_s/\omega=0.01\bar{u}/V$ have, however, been calculated in consistent units of $\bar{u}$ and V.

The prevailing values of the stage criterion θ have been added, together with the maximum and mean grain sizes of the bed.

In summary of the comparative transport rates (table 1), the predicted rates are within a factor of 1.5, either way, of the measured rates in 49 percent of the data sets and within a factor of 2 in 65 percent of the data sets. Moreover the overall geometric mean of all the 146 discrepancy ratios is as near parity as 0.73. When all the uncertainties are considered this measure of agreement is very promising.

The discrepancies given in table 1 are analysed in figure 14 according to river and gaging station. There is, as figure 14 shows, a marked correlation between the discrepancies and their relevant stations. Although for most of the data the points are significantly concentrated close to the parity line, the results from some stations, for example, Colorado River of the West at Lees Ferry, Ariz., and Colorado River of Texas at Columbus, Tex., are very erratic.

It should be remembered that energy effects calculated from data obtained from a single cross section of a river are likely to be unrepresentative. In addition most of the gaging stations involved were permanently sited for the original and simpler purpose of gaging water discharge only; for that purpose the effects of local energy interchanges are immaterial. The Lees Ferry station, for instance, is sited just downstream of an abrupt widening of the river channel.

The discrepancies shown above the parity line in figure 14 indicate too large a predicted value; these discrepancies, however large, can readily be explained by concurrent infilling of a local scour, by a general dearth of suspendable material, or by the flow stage being subcritical. In many plots where the predicted rates are several times too large, the stage as indicated by θ

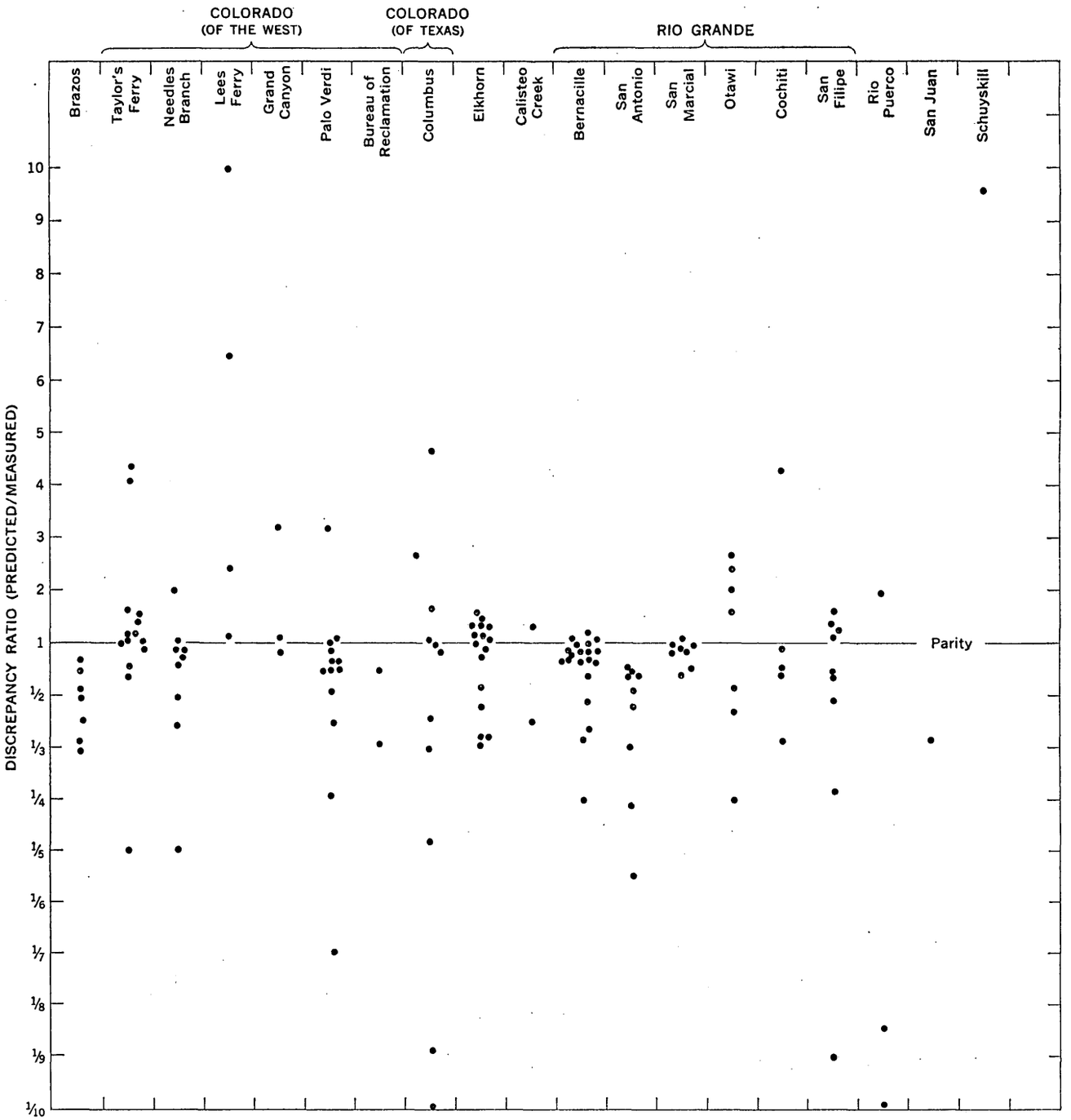

FIGURE 14.—Transport-rate discrepancies (predicted/measured), from table 1, grouped according to river and station.

either is below the critical value or may well have been had the actual bed-surface conditions been better known. Big discrepancies in this direction do not occur when θ is large.

The many large discrepancies in the other direction indicate too small a predicted value and are of more interest. A search for their probable cause led me to inspect the recorded size distributions of the sampled material transported, for some common abnormality.

While the sampler is lowered through the river to final contact with the bed and is then withdrawn, it seems inevitable that some of the coarser bedload grains become included in the integrated sample. The proportion in most samples may be small, but in the presence of large-scale bed features such as boulders, gravel bars, and old bridge debris it may be very appreciable.

The inclusion of bedload transported by another mechanism, and therefore likely to have a different

size distribution, should, it seem reasonable to suppose be manifested in the combined size distribution.

The conventional integrated percentage-less-than method of presentation of size distributions discloses but little useful detail. Indeed it is designed to smooth out irregularities. When, however, the distribution is converted back into its original grade proportions p, and these are plotted as log p against log D, distinguishing features can readily be spotted.

Exceptionally low predicted transport rates appear to be associated with size distributions having an actual or inferable second hump toward the larger end of the size scale. Conspicuous examples are shown in figures 15A and B. When these curves are adjusted by the removal of the second hump and the appropriate increase of the remaining p values, the summation ΣpV_p is reduced to the extent that the predicted value of $0.01\bar{u}/V$ is increased to the right order of magnitude.

In some plots the second hump is merged into the main one to the extent that its presence is difficult to distinguish. Figure 15C gives an example. Here again, a reasonable adjustment based on the rather slight indications is found to remove the discrepancy in the transport rates.

It should be a simple matter to test this hypothesis by duplicating the sampling. If a sample taken over the full depth, to contact with the bed, were to show the second hump as in figures 15A and B, owing to the inclusion of bedload material, another sample taken on the same occasion down to say only two-thirds of the depth should show the second hump to be absent or considerably reduced.

In this connection, although the majority of the discrepancies in table 1 are comparatively small, those in the direction of too low a predicted value are markedly preponderant. In view of the close agreement of the laboratory data, it would seem advisable, before attempting to apply some empirical correction to the coefficients of equation 20, to investigate the extent to which responsibility for this general tendency can be attributed to the inevitable inclusion of coarser bedload material in the samples of supposedly suspended loads.

Considerably clearer inferences could be drawn from distribution graphs such as those of figure 15 had the size analyses been made in grade intervals of $\sqrt{2}$, instead of the wider intervals of 2 and sometimes 4.

Some further points are noteworthy in connection with table 1. Although the θ values shown cannot be regarded as precise, they do appear to indicate that in the types of river sampled, at any rate, conditions usually are those of the high transport stages to which the present theory is applicable.

Since the present theory takes both modes of sediment transport into consideration, it should be applicable to rivers which transport relatively large materials—pebbles, gravels, and boulders—mainly as bedload. None of these types of river, however, are included in the table, for the reason that no data are available owing to lack of means of measurement. Hence the bedload part of the theory remains untestable except by Gilbert's laboratory experiments done at clearly inadequate flow depths and over a too limited range of transport stages.

Lastly, the need is evident for accurate determinations of the true-energy slopes of rivers.

COMPARISON OF RIVER TRANSPORT DATA WITH DATA FOR WIND-TRANSPORTED SAND

From the viewpoint of general physics, a broad theory of the present kind would be expected to be consistent with the facts over a still wider field. For it is contrary to experience that Nature restricts the operation of her basic principles to particular phenomena, such as the transport of solids by a particular fluid. If the theory is soundly based, therefore, it should be consistent with evidence on the transport of windblown sand.

This evidence indicates in the first place that the transport of sand—as opposed to fine dust—over the ground is by the bedload mechanism alone, suspension by air turbulence being negligible over the range of wind speeds commonly experienced. Hence the first term of equation 20 should alone be operative.

Owing to the very low dynamic viscosity of air, the conditions of the bedload motion are wholly inertial; so tan α should be constant at its lower value.

The theory would therefore predict that the transport rate of a given windblown sand should, to a close approximation, be proportional to the available power.

The quantitative data from wind-tunnel experiments is definite on this point (Bagnold, 1941; Zingg, 1950). The transport rate is indeed proportional to the power. So to this extent the theory is entirely consistent.

CONCLUSION

The foregoing theory constitutes an attempt to explain the natural process of sediment transport along open channels quantitatively, by reasoning from the general principles of physics and from the results of certain critical experiments. General relationships have been derived independently of any quantitative data drawn from experiments on channel flow. To this extent the theory is rational rather than empirical.

Consideration has been confined to transport conditions at the higher stages of flow. For here the process appears to be much simpler than over the lower, transitional stages. An understanding of this simpler process is directly relevant to much of riverflow, and should be relevant indirectly to the more difficult problems presented by the lower, transitional stages.

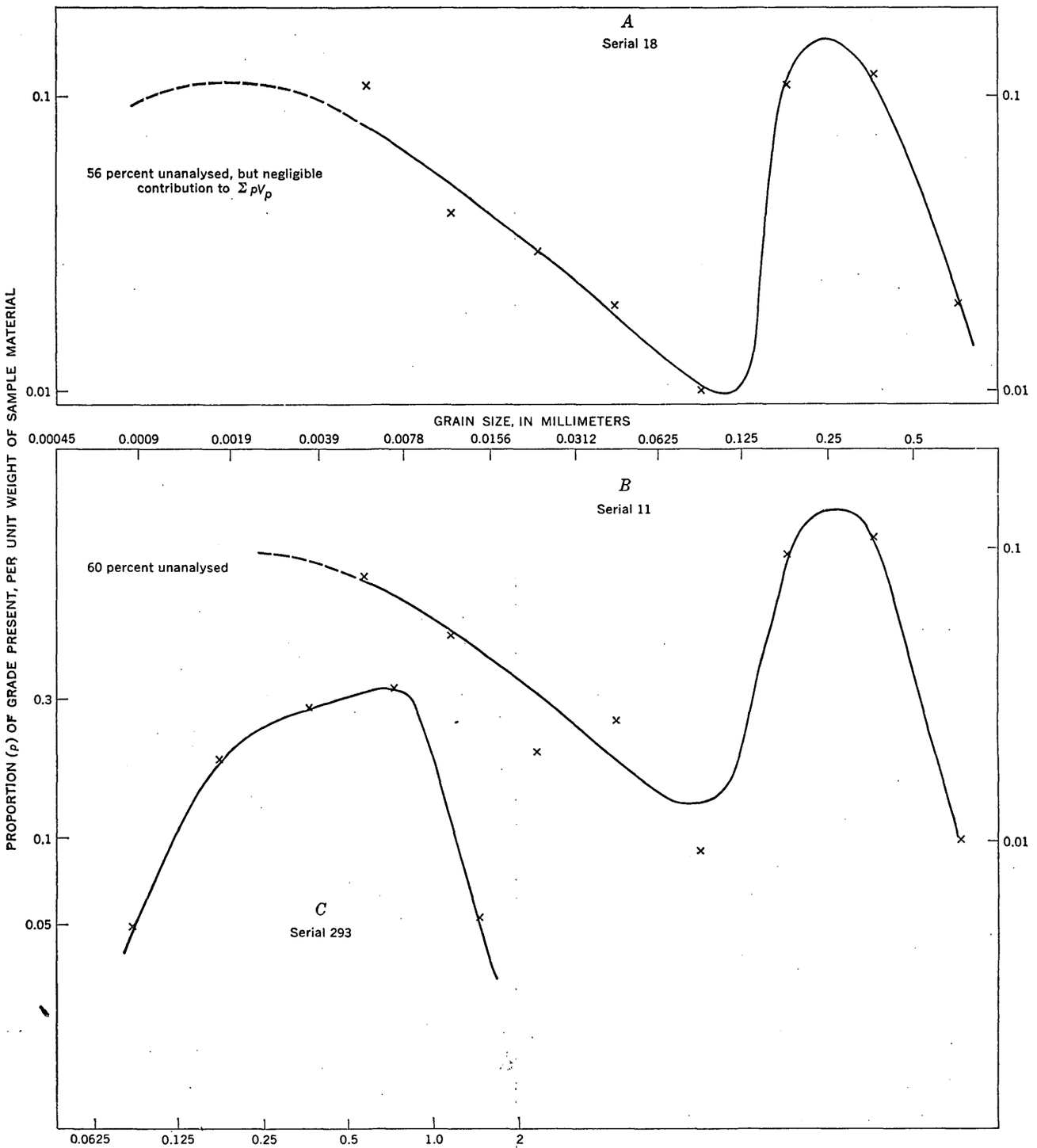

FIGURE 15.—Examples of anomalous size distributions of assumedly suspended river loads, associated with anomalous transport rates predicted from them (suggesting that the sampling had included a proportion of coarser bedload material).

Within the flow region considered, the derived relationships are, I believe, fairly and evenly consistent with the available facts over a range of conditions far wider than for any previous theory.

Wide consistency of this kind tests the general form of a theoretical relationship in a way that consistency over a narrow range of conditions connot do. If the general form appears sound, the relationship is worth additional study by others who may modify the parameters in the light of further factual knowledge to bring the relationship into closer approximation everywhere without detriment to its generality.

No theoretical results can, however, be properly tested unless the facts against which they are tested are

themselves both adequate and certain. If the facts, are in doubt, then a fair approximation is all that can be expected. Many serious factual inadequacies and uncertainties in the existing knowledge about sediment transport have already been pointed out. The majority could undoubtedly be removed by experimental researches of a critical kind, if these were imaginatively and scientifically designed and carried out for this specific purpose only, regardless of either convention or immediate practical utility. Given adequate facilities, each of the researches I have in mind should be capable of completion within a short period of say 2 years. Continued tolerance of longstanding factual uncertainties cannot but have an adverse effect on the status of research in this field.

The most serious factual inadequacy in the field of sediment transport is, I suggest, our lack of data on the unsuspended transport of bedload by a turbulent fluid. The reason is of course our inability to separate this transport experimentally from a concurrent transport in turbulent suspension. Consequently we cannot check theoretically predicted transport rates by either mechanism separately. So any theory must extend to cover the prediction of both transport rates before any verification is possible.

This difficulty remains insuperable so long as the belief prevails that bedload, although unsuspended, is yet somehow activated and transported by the agency of turbulence. The present theory however denies this belief, on the direct visual evidence that the saltating motion characteristic of bedload transport persists also under laminar flow in the entire absence of turbulence. The bedload transport relationship it derives is applicable both to turbulent and laminar conditions.

This immediately opens the possibility that the transport of bedload can be studied quantitatively under conditions of laminar flow in a way that is impossible under practical turbulent conditions except within the narrow range of large grains at very low flow stages.

Unfortunately no quantitative experiments on sediment transport by laminar flow have ever been done; for on the above belief, such experiments would be irrelevent and unpractical. For the same reason even simple qualitative experiments have been so rare that few if any present-day workers have had opportunity to observe the reality of transport by laminar flow and the closeness of its similarity to transport by turbulent flow.

It is hard to avoid the conclusion that progress in the field of sediment transport has been retarded by a refusal to appreciate the significance of experimental results which may appear superfically to be unpractical.

REFERENCES

Bagnold, R. A., 1941, Physics of blown sand: New York, William Morrow.

——— 1954, Experiments on the gravity-free dispersion of large spheres in a Newtonian fluid under shear: Royal Soc. [London] Proc. A 225, 49.

——— 1955, Some flume experiments on large grains but little denser than the transporting fluid, and their implications: Inst. Civil Engineers Proc., Pt. 3.

———1956, Flow of cohesionless grains in fluids: Royal Soc. [London] Philos. Trans., v. 249, p. 235–297.

Barton, J. R., and Lin, P. N., 1955, A study of sediment transport in alluvial channels: Fort Collins, Colorado State Univ., Agr. and Mech. Coll. Rept. 55, JRB 2.

Brooks, N. H., 1957, Mechanics of streams with movable beds of fine sand [Includes experiments by V. A. Vanoni and N. H. Brooks, and by G. Nomicos]: Am. Soc. Civil Engineers, v. 83, no. HY 2.

Durand, R., 1952, Proceedings of colloquium on hydraulic transport of coal: London Natl. Coal Board.

Gilbert, G. K., 1914, The transportation of débris by running water, based on experiments made with the assistance of E. C.Murphy: U.S.Geol. Survey Prof. Paper 86, 263 p.

Irmay, S., 1960, Accelerations and mean trajectories in turbulent channel flow: Am. Soc. Mech. Engineers Trans., December.

Knapp, R. T., 1938, Energy balance in stream flows carrying suspended load: Am. Geophys. Union Trans., p. 501–505.

Laufer, J., 1954, The structure of turbulence in fully developed pipe flow: Natl. Advisory Comm. for Aeronautics Rept. 1174.

Laursen, E. M., 1957, An investigation of the total sediment load: Iowa State Univ. Inst. Hydrol. Research.

Prandtl, L., 1952, Essentials of fluid dynamics: London, Blackie & Son.

Reynolds, Osborne, 1885, On the dilatancy of media composed of rigid particles in contact: Philos. Mag., 5th ser., v. 20, p. 469–489.

——— 1895, On the dynamic theory of viscous incompressible fluids and the determination of the criterion: Roy. Soc. [London] Philos. Trans., v. 186 A., p. 123.

Rubey, W. W., 1933, Equilibrium conditions in débris-laden streams: Am. Geophys. Union Trans., 14th Ann. Mtg., p. 497–505.

Shields, A., 1936, Anwendung der Änhlichkeitsmechanik und der Turbulenzforschung auf die Geschiebebewegung: Berlin Preuss, Versuchsanstalt fur Wasser, Erd und Schiffbau, no. 26.

Simons, D. B., Richardson, E. V., and Albertson, M. L., 1961, Flume studies using medium sand (0.45 mm): U.S. Geol. Survey Water-Supply Paper 1498–A, 76 p.

Townsend, A. A., 1956, The structure of turbulent shear flow: Cambridge Univ. Press.

U.S. Inter-Agency Committee on Water Resources, 1958, Some fundamentals of particle size analysis: U.S. Inter-Agency Comm. Water Resources, Sub-Comm. Sedimentation Rept. 12, 55 p.

——— 1961, River basin maps showing hydrologic stations: U.S. Inter-Agency Comm. Water Resources, Sub-Comm. Hydrology, Map 59.

Velikanov, M. A., 1955, Dynamics of channel flow—v. 2, Sediments and the channel [3d ed.]: Moscow, State Publishing House for Tech.-Theoretical Lit., p. 107–120 [In Russian].

Zingg, A. W., 1950, Annual report on mechanics of wind erosion: U.S. Dept. Agriculture Soil Conserv. Service.

U.S. GOVERNMENT PRINTING OFFICE:1966